CHEN, XUEJIN, M.S. Mathematical Models for the pH Dependence of Oxygen Evolution under Fluoride Inhibition and Effects of Nitrite on Oxygen Evolution in Photosystem II. (2008)
Directed by Dr. Alice E. Haddy. 129 pp.

Photosynthesis produces dioxygen at photosystem II (PSII), which is located in the thylakoid membrane of plant chloroplasts. Chloride (Cl^-) is required for oxygen evolution activity and other anions are known to activate or inhibit O_2 evolution. In this study, the inhibitory effects of fluoride (F^-) and nitrite (NO_2^-) were investigated to gain insight into the requirement for Cl^-. The way the pH dependence is affected might reveal the type of residue that the Cl^- binds to. In the first part of the study, a simplified model followed by a comprehensive kinetic model for the pH dependence of O_2 evolution under F^- inhibition in intact PSII was built based on the data of T. Delaney Santoro from the same lab, which included several F^- concentrations. The results show that the comprehensive model fit the experiment data quite well. The dissociation constants between enzyme E and its complexes EH^+ and $E(H^+)_2$, pK_1 and pK_2, were found to be 5.1 and 7.2. The inhibition constants of F^- binding to E, EH^+ and $E(H^+)_2$ were 15.8 mM, 381 mM and 2.0 mM, respectively. In the second part of the study, the NO_2^- dependence of O_2 evolution by PSII was characterized. The investigation showed that NO_2^- activated

O_2 evolution at low concentrations and inhibited at the higher concentrations in both NaCl-washed PSII and intact Cl^- depleted PSII. This characteristic of nitrite is similar to that of iodide (I^-) and nitrate (NO_3^-). The kinetics of NO_2^- action in O_2 evolution was modeled as substrate inhibition, in which NO_2^- activates from the Cl^- site and inhibits from a second site. It also suggested that the inhibition due to NO_2^- in PSII lacking extrinsic subunits PsbP and PsbQ was primarily uncompetitive with uncompetitive inhibition constant K_i' of 0.60 mM, while the NO_2^- inhibition in intact PSII was probably in an uncompetitive mode with inhibition constant K_i' of 14 mM. However, the competitive inhibition constants K_i for both types of PSII were not well determined due to large error in the data. The Michaelis constants K_m for NO_2^-, Cl^- and NO_3^- were found to be 0.33 mM, 0.54 mM and 0.16 mM for intact Cl^- depleted PSII. The K_m values for NO_2^-, Cl^-, and NO_3^- without substrate inhibition were 2.1 mM, 5.0 mM, and 5.5 mM for NaCl-washed PSII, respectively. These values are fairly close and all are within the error range for each type of PSII.

MATHEMATICAL MODELS FOR THE pH DEPENDENCE OF OXYGEN EVOLUTION UNDER FLUORIDE INHIBITION AND EFFECTS OF NITRITE ON OXYGEN EVOLUTION IN PHOTOSYSTEM II

by

Xuejin Chen

A Thesis Submitted to
the Faculty of The Graduate School at
The University of North Carolina at Greensboro
in Partial Fulfillment
of the Requirements for the Degree
Master of Science

Greensboro
2008

Approved by

Alice E. Haddy
Committee Chair

APPROVAL PAGE

This thesis has been approved by the following committee of the Faculty of The Graduate School at The University of North Carolina at Greensboro.

Committee Chair_____
Alice E. Haddy

Committee Members_____
Nadja B. Cech

_____
Jason J. Reddick

_____
Date of Acceptance by Committee

_____
Date of Final Oral Examination

ACKNOWLEDGEMENTS

This research was completed under the instruction of Dr. Alice Haddy of the Department of Chemistry and Biochemistry in The University of North Carolina at Greensboro. I should like to give my special thanks to her for what she has done for me. She has not only been my advisor for five years, but also given me tons of information, support and help during my studies in the school. Without her precious advice and help, the research would be much more difficult for me to finish. I also would like to give my sincere appreciation and thanks to Dr. Nadja Cech and Dr. Jason Reddick for their advice and suggestions on both the research proposal and the thesis.

Many data, provided by Dr. Alice Haddy, were collected by Mr. T. Delaney Santoro and Mr. Madhu Kumar. I wish to thank them for their work which has been a benefit to me. Thanks are extended to Mr. Xiaoming Li for the chloride-depleted PSII membranes that he made. His samples made the research go smoothly and faster.

TABLE OF CONTENTS

Page

LIST OF TABLES

Page

LIST OF FIGURES

Page

Page

CHAPTER I

INTRODUCTION

It has been well known that photosynthesis produces oxygen. Almost all molecular oxygen or dioxygen we breathe is produced by photosynthesis. As a plentiful energy source, the sun gives off light that is absorbed by plants. Plants transform light energy into chemical energy in the process that converts water into oxygen. This process is a part of the photosynthesis. Chloroplasts are the subcellular organelles where photosynthesis occurs, and many molecular and biochemical details of photosynthesis are known. However, the precise molecular mechanism of oxygen evolution is still unclear.

The oxygen-evolving complex (OEC) in photosystem II (PSII) can extract electrons from water and produce molecular oxygen as a byproduct. Scientists have found that different kinds of anions and molecules have different effects on the function of the OEC: anions such as chloride (Cl^-) are essential and accelerate the oxygen evolution process;[1] but fluoride (F^-), amines, and some other anions and molecules inhibit this process.[2] The topic of Cl^- effects on oxygen evolution of PSII is still of interest in the field.[3] The effects of other anions on the oxygen evolution process have also been studied by scientists. For

instance, anions like Br^- activate the oxygen evolving process, but a few chemicals and anions such as F^-, CH_3COO^-, N_3^-, Tris, NH_3, etc. are inhibitory to the process. Some studies confirmed that I^- and NO_3^- activated the oxygen evolution process at lower concentrations and acted as an inhibitor at higher concentrations in intact Cl^- depleted PSII and NaCl-washed PSII.[4, 5] Meanwhile, the pH of the medium in PSII also has effects on the oxygen producing process.[6]

This research focused on two topics. The first topic was the mathematical models for the pH dependence of oxygen evolution rate under fluoride inhibition in PSII. The relationship between anion effects and pH effects is complex. The pH effects are often related to proton transfer and/or H-bond systems at the catalytic site. Anions may promote the correct participation of the proton in catalysis. So far, the mathematical models of anion inhibition with pH dependence have not been well developed. The second topic was the effects of NO_2^- on the oxygen evolution rate in PSII. Some previous studies suggested that NO_2^- may have similar effects as I^- on the oxygen evolution rate of PSII with both activation and inhibition characteristics.[4] The mode of the effect of nitrite (NO_2^-) on oxygen evolution has not previously been fully studied.

CHAPTER II

BACKGROUND AND LITERATURE REVIEW

Photosynthesis is a process that uses light energy to convert carbon dioxide and water into carbohydrates and molecular oxygen. The overall process can be expressed as

$$6CO_2 + 6H_2O \rightarrow C_6H_{12}O_6 + 6O_2 \qquad \textbf{Reaction 1}$$

where $C_6H_{12}O_6$ represents a sugar molecule such as glucose. The reaction requires energy to proceed ($\Delta G^{\circ\prime} = 2870$ kJ/mol).[7] Photosynthesis can be broken down into two sets of reactions: the light reactions and the dark reactions.[8]

Overall Light Reactions

$$2H_2O \rightarrow O_2 + 4H^+ + 4e^- \qquad \textbf{Reaction 2}$$

Overall Dark Reactions

$$CO_2 + 4H^+ + 4e^- \rightarrow (CH_2O)_n + H_2O \qquad \textbf{Reaction 3}$$

These reactions are carried out in chloroplasts that can be found in mesophyll cells under the surface of plant leaves. Chloroplasts enclose a network of thylakoid membranes, which contain all of the proteins and pigments (chlorophylls and carotenoids) required for photosynthesis. Light-trapping pigments along with associated proteins are

organized into large membrane-embedded complexes called photosystems. Each photosystem is responsible for absorbing a light photon and converting some of its energy into a chemical form.[9]

Photosystems

Two kinds of photosystems are involved in photosynthesis in plants: photosystem I (PSI) and photosystem II (PSII). PSI has light absorbance up to 700 nm and PSII has light absorbance up to 680 nm. The two systems are linked in a series to carry out the electronic transfer of the light reactions (Figure 1). The overall reactions of the photosystems are

$$\text{PSII:} \quad 2H_2O + 2Q \xrightarrow{\text{light}} O_2 + 2QH_2 \qquad \textbf{Reaction 4}$$

$$\text{PSI:} \quad NADP^+ + H^+ + 2PC_{red} \xrightarrow{\text{light}} NADPH + 2PC_{ox} \qquad \textbf{Reaction 5}$$

in which PC is plastocyanin.

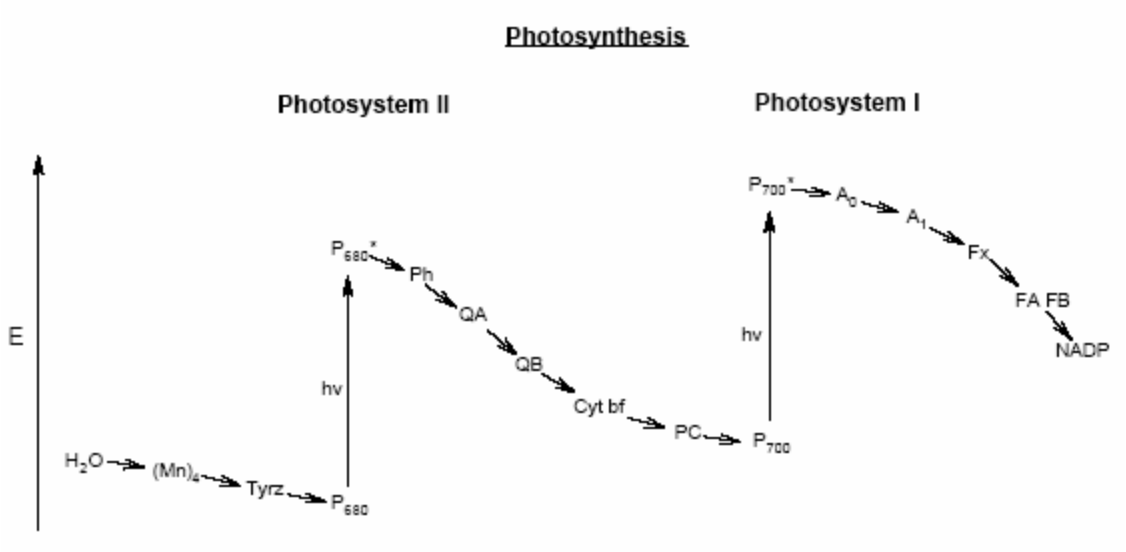

Figure 1 Diagram of photosystems [10]

Electrons transfer from H_2O to QH_2 in PSII while electrons transfer from PC_{red} to NADPH in PSI. PSII plays the key role in oxygen evolution. The oxygen evolution process depends on the light harvesting complexes, the photochemical reaction center, and the oxygen-evolving complex. In PSII, after light energy is absorbed by light harvesting complexes containing chlorophylls and carotenoids, the excitation energy is transferred to the photochemical reaction center for charge separation. At the same time, oxidizing equivalents in the oxygen-evolving complex are accumulated and four of the equivalents are used to convert two molecules of water to one molecule of oxygen. Several electron transfer components are involved in the process of photochemical reaction in PSII. In the photochemical

reaction, P680 (PSII reaction center chlorophyll) is excited upon light absorption and transfers an electron to pheophytin (Ph, a chlorophyll molecule without magnesium). The electron is then transferred to plastoquinone Q_A. Ultimately, two electrons are sent to a second plastoquinone Q_B, with concurrent binding of two protons. After leaving PSII, the reduced plastoquinone, plastoquinol (QH_2), diffuses through the membrane and interacts with cytochrome b_6f (Cyt b_6f), which is a membrane-bound complex of cytochromes and iron-sulfur proteins. Cyt b_6f catalyzes the transfer of the electrons to plastocyanin (PC) which passes the electrons to the P700 reaction center of PSI.[7, 10]

Protein Subunits of PSII

PSII is a multi-protein complex containing intrinsic subunits including D1, D2, CP43, CP47, psbl gene product, cytochrome $b_{559,}$ and extrinsic subunits including 33 kDa, 23 (or 24) kDa, 17 (or 18) kDa, 12 kDa, and Cytochrome b_{550}, depending on the species (Figure 2). The crystal structure of oxygen-evolving PSII has been studied by Zouni et al. in 2001,[11] by Kamiya et al. in 2003,[12] and by Loll et al. in 2005.[13] The intrinsic subunits are made up mostly of α-helical transmembrane structure. D1 (PsbA) and D2 (PsbD) subunits are the core of the PSII reaction center, and bind

a variety of cofactors. Most electron transfer occurs in the D1 and D2 proteins. CP47 (PsbB) and CP43 (PsbC) transfer excitation energy from the light harvesting chlorophylls to the chlorophylls in the PSII reaction center. Cyt b_{559} (PsbE and PsbF) is a redox center.[14]

The extrinsic subunits enhance oxygen evolution activity at physiological concentrations of inorganic cofactors, and appear to regulate the access of water and ions at the OEC. Without the 33 kDa (PsbO) subunit, the manganese cluster is unstable under low chloride conditions. Removal of the 23 kDa (PsbP) and 17 kDa (PsbQ) proteins increases the amount of calcium and chloride required for optimal oxygen evolution. Therefore, these two subunits function in the regulation of Cl^- and Ca^{2+} in OEC. It is known that all PSII contains the 33 kDa protein. However, the higher plant PSII also contains the 17 kDa and 23 kDa subunits, whereas the cyanobacteria PSII has the Cyt c_{550} (PsbV) and 12 kDa (PsbU) subunits.[11, 15, 16] The presence of the 33 kDa subunit is a necessary condition for the binding of the 17 and 23 kDa subunits on the PSII membrane. They are the three largest extrinsic subunits. Washing with 1.0 M NaCl can remove the 17 and 23 kDa subunits, while washing with 1.0 M $CaCl_2$ removes all three subunits.[1] The overall architecture for OEC is now well known.[17] Figure 2 presents a schematic depiction of the subunit arrangement in PSII.

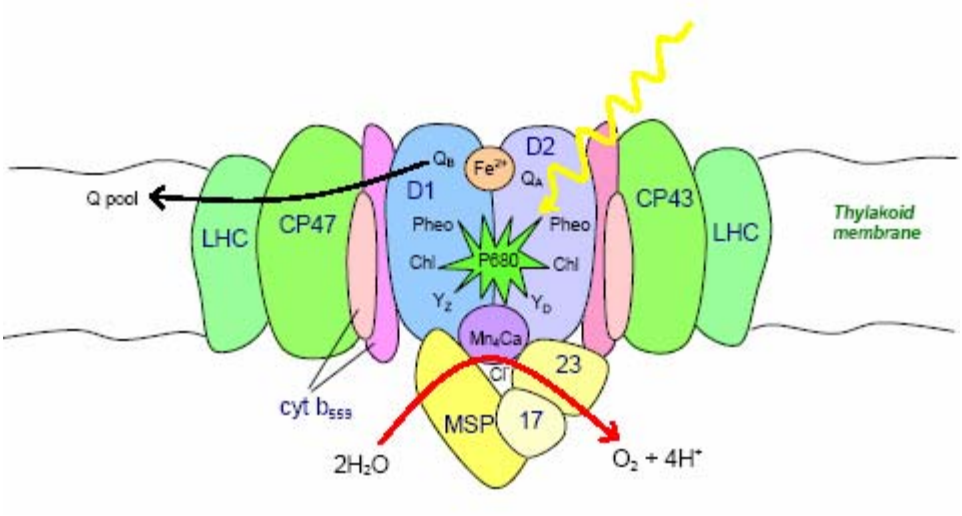

Figure 2 Schematic structure of PSII (provided by Alice Haddy)

Figure 3 shows a schematic view of the OEC based on the finding of Ferreira et al.[17] In the figure, residues Q165, H190, D170, E333, D61, E65, E189, H337, H332 and D342 as well as TyrZ and C-term are located on the D1 intrinsic subunit; residues E312 and K317 are on the D2 intrinsic subunit; residues R357 and E354 are on the CP43 intrinsic subunit; X_{11}, X_{21} and X_{22} are possible substrate water bound to Mn4 (X_{11}) and to Ca^{2+} (X_{21} and X_{22}). W indicates the possible water molecules that are not visible at the current resolution. The dotted lines are hydrogen bonds.

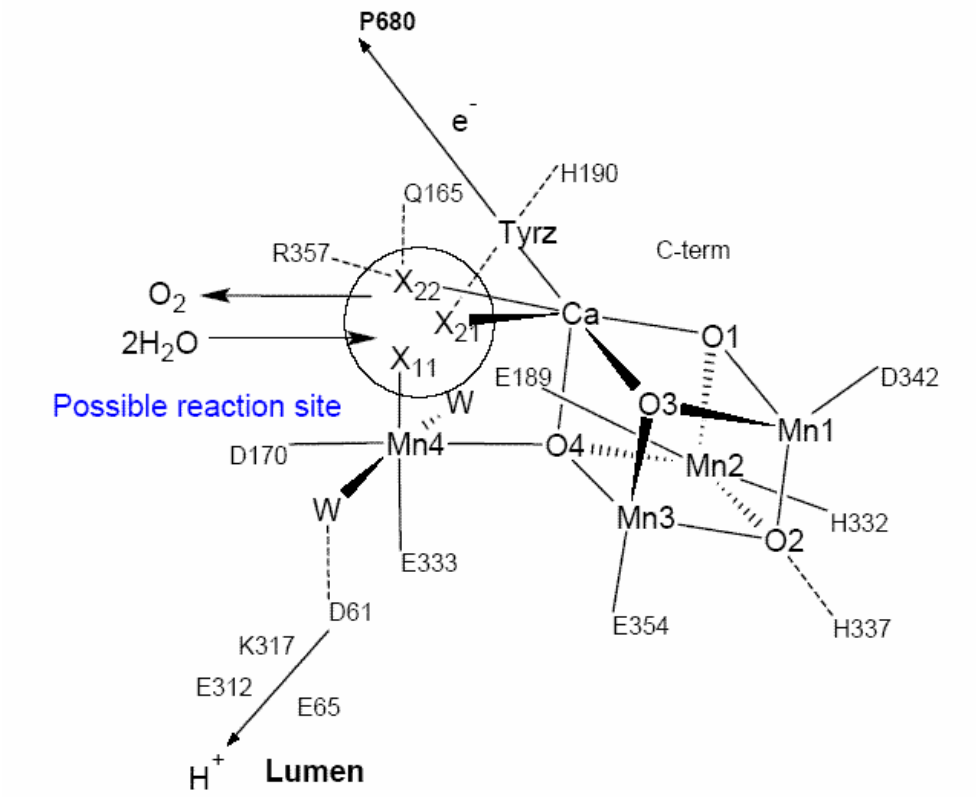

Figure 3 Schematic view of the OEC [17]

Franzén and coworkers studied the roles of the extrinsic subunits in PSII using EPR.[16] Their research showed that removal of the 16 and 24 kDa proteins by treating with 1 M NaCl solution inhibited the oxygen evolution activity, but rapid electron transfer to Z^+ was still observed. Removal of the 33 kDa subunit with $MgCl_2$, however, almost completely inhibited the oxygen evolution process, indicating that the 33 kDa subunit was necessary for oxygen evolution. Many other papers also addressed this topic.

Oxygen Evolution Process

After P680 is oxidized to $P680^+$, it is electron deficient and regains electrons from water. A protein containing a cluster of four Mn atoms accepts the electrons from water. This Mn cluster cycles through five oxidation states in what is called the Kok cycle or S-state cycle (Figure 4), and passes the electrons to $P680^+$ via an intermediate tyrosine radical ($Y_z\cdot$).[7]

Photon absorption and electron transfer from P680 (or charge separation) cause formation of $P680^+$ which then oxidizes Y_z to $Y_z\cdot$. Then $Y_z\cdot$ extracts an electron from the OEC and induces the $S_0 \rightarrow S_1$ transition. Subsequent photon absorptions by P680 drive the $S_1 \rightarrow S_2$, the $S_2 \rightarrow S_3$ and the $S_3 \rightarrow S_4$ transitions, where each is one oxidation step. The S_4 state, the highest oxidation state, is unstable and releases dioxygen, resetting the cycle.[18]

There are two charge recombination processes in PSII, one involves the S states of the water-oxidizing complex at the electron donation side and the other is in the plastoquinone molecules (Q_A and Q_B) at the electron acceptor side.[19]

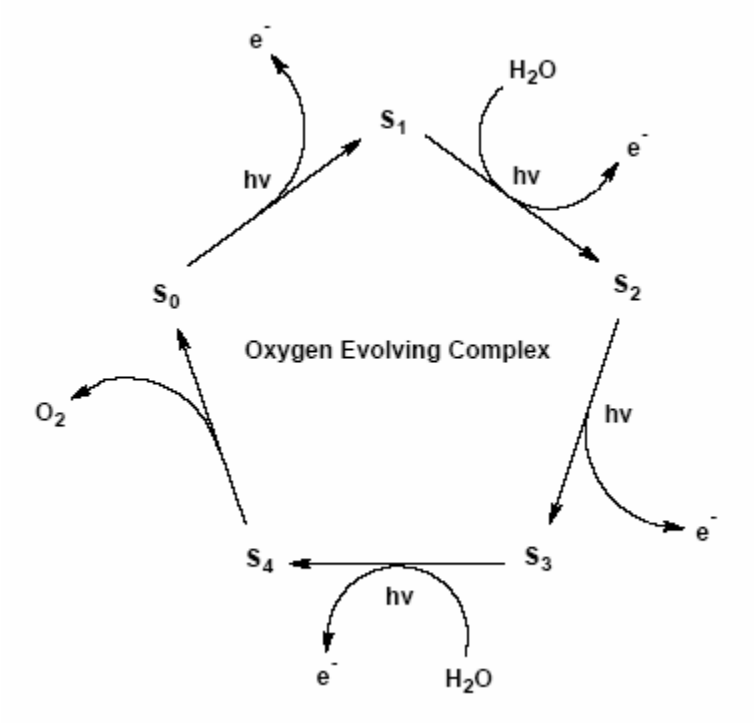

Figure 4 OEC S-state cycle or Kok cycle

So far, two water oxidation mechanisms have been proposed, the metal cluster mechanism and the metallo-radical mechanism.[18, 20] The metal cluster mechanism has been described by Ferreira et al. while the research on metallo-radical mechanism was described by Hoganson and Babcock.[17, 21]

Effects of Inorganic Cofactors on PSII

Manganese, calcium and chloride are three primary inorganic cofactors of PSII that are vital to oxygen evolution. Four Mn ions are needed for the conversion of

water into oxygen. These Mn ions comprise the manganese complex or cluster that is the core of the OEC.[17, 21]

Calcium, a cationic activator of O_2 evolution, is required at the oxidizing side of PSII, and is now required to be a part of the manganese cluster as Mn_4Ca.[14, 22, 23] Calcium-depleted PSII loses oxygen evolving ability. Without the 17 and 23 kDa proteins in PSII membrane (NaCl-washed PSII), a higher amount of Ca^{2+} is needed for maximal oxygen evolution activity. Calcium is essential for the Kok cycle to proceed beyond the S_2 state. A wide range of other metal ions has been tested to replace Ca^{2+}, however, only strontium (Sr^{2+}) can promote OEC activity, but with about 50% as much as that of Ca^{2+}. It was found that the substitution of lanthanides for Ca^{2+} inhibited oxygen evolution activity, which indicates that the binding site of Ca^{2+} is the active site of the O_2 evolving reaction. Analyses and studies strongly support the viewpoint that there is one Ca^{2+} ion binding in the OEC and that one or more Ca^{2+} ions are bound to other sites of PSII membranes. Recent research has showed that Ca^{2+} resides near the Mn cluster at a distance of 3.4-3.5 Å, and is a part of the Mn_4-Ca cluster in the OEC. Most recently, it was confirmed by X-ray diffraction studies that Ca^{2+} was ligated at least partly by amino acid side chain residues of the 33 kDa subunits (PsbO).[23, 24] Another binding site for Ca^{2+} is in

the antenna protein ensemble, and the other sites are unknown. So far as we know, none of the 17 and 23 kDa extrinsic subunits can retain tightly bound to Ca^{2+}.

As an activator of oxygen evolution, chloride plays an important and specific role in the regulation of redox reaction in PSII.[14, 25] Cl^- activation has been widely studied and is still a subject of active experimentation. PSII samples without Cl^- show inactivation of the OEC. Chloride facilitates oxidation of the Mn cluster by the Tyr-Z^+ radical through its activation effect.[26] The maximal oxygen evolution activity of PSII can be reversibly decreased by the depletion of Cl^- using a variety of methods such as washing with Cl^- free buffers, washing at alkali pH and dialysis in the presence of other anions. PSII membranes lacking the 17 and 23 kDa proteins can be easily depleted of Cl^-. These PSII membrane preparations can still reach S_1 and S_2 states in the absence of Cl^-, indicating that chloride apparently binds at the S_2 or earlier S state. The depletion of it inhibits the advancement of the OEC beyond S_2, that is, Cl^- is necessary for the S-cycle going beyond S_2 state. In fact, it is required for the $S_2 \rightarrow S_3$ transition, and is also required for the transition from S_3 to S_0. Like calcium, however, the mechanistic details for the way that Cl^- affects the redox reaction in the OEC

remain obscure. Chloride has been proposed to bind to the manganese cluster or a site very close to manganese.

Effects of Other Anions and Amines on Oxygen Evolution

Anions and amines can have a variety of effects on the oxygen evolving process ranging from activation to inhibition. Cl^-, Br^-, I^- and NO_3^- activate the oxygen evolving process. Also, Lindberg et al. found that bromide binds in a manner similar to that of Cl^- in PSII and activates oxygen evolution,[27] and that removal of the slowly exchanging chloride lowers the stability of PSII, which means that Cl^- is vital for oxygen evolution activity.[28] On the other hand, F^-, NH_3, amines, N_3^- (azide), Tris etc. inhibit the process. The mechanism for inhibition can be competitive with Cl^- activation and/or uncompetitive, depending on the ion type. Fluoride inhibits the oxygen evolution process completely by preventing the $S_2 \rightarrow S_3$ transition by Cl^- competitive inhibition. It was found that declining enzymatic activity of the PSII reaction center resulted from increasing the F^- concentration in an EPR study of the signals from the Mn_4-Ca cluster.[29] N_3^- inhibits oxygen evolution activity because it is a competitor of Cl^-.[30, 31] However, some ions such as I^- can be either activators or inhibitors under certain conditions.[2] I^- inhibits oxygen evolution from an uncompetitive site, but

activates the process from the Cl^- site.[4] The overall order of oxygen evolution suppression or inhibition ability was reported as NO_3^- < I^- < F^- < CH_3COO^-.[32]

Oxygen Evolution Rate in PSII

Intact PSII preparations contain membrane fragments with membrane-embedded PSII complexes of complete sets of subunits. They can be prepared from spinach thylakoid membranes or other plants.[33] Intact PSII shows high oxygen evolution activity with little or no apparent dependence on Ca^{2+} or Cl^-. It is difficult to remove Cl^- from intact PSII, since the best Cl^- depletion methods still leave 30% or more activity. By removing the extrinsic 17 and 23 kDa proteins from the intact PSII, the PSII complexes may lose most of their oxygen evolution activities in the absence of Ca^{2+} or Cl^-. These preparations are often called “salt-washed PSII” or NaCl-washed PSII, since they are made from the treatment of intact PSII with 1-2 M NaCl solution thereby removing the 17 (or 18) and 23 (or 24) kDa subunits.[34] Calcium and chloride are required for NaCl-washed PSII to maintain oxygen evolution activity because the 17 and 23 kDa subunits probably regulate the local concentrations of Ca^{2+} and Cl^-. To help understanding the details of anion activation and inhibition, intact and NaCl-washed PSII preparations can be compared. The use of NaCl-washed PSII

facilitates Cl^- depletion, which will help to reveal the real tendencies and effects of Cl^- and other anion activators and inhibitors on the oxygen evolution activity.

pH Dependence of the Oxygen Evolution in PSII

The pH of the medium has important effects on the oxygen evolution activity of PSII as for other enzymes. The oxygen evolution rate increases with pH until a peak range around pH 6.3-6.5 is reached. At higher pHs, the oxygen evolution rate decreases with the pH value.[6] Most enzymes also show this type of pH dependence with some optimal pH. The pH effect can be expressed in the following reactions.

$$E(H^+)_2 \overset{K_1}{\rightleftharpoons} EH^+ + H^+ \overset{K_2}{\rightleftharpoons} E + 2H^+ \qquad \textbf{Reaction 6}$$

in which E is the enzyme. Here EH^+ is the active form, but $E(H^+)_2$ and E are not. The kinetic model can be written as

$$A = \frac{A_{max}}{1 + \frac{[H]}{K_1} + \frac{K_2}{[H]}} \qquad \textbf{Equation 1}$$

where A is the oxygen evolution activity, A_{max} is the maximum activity when all enzyme is in the EH^+ complex form, K_1 and K_2 are proton dissociation constants, and [H] stands

for the concentration of H^+. The presence of other ions, however, can affect the apparent pK_as.

Kinetics of Oxygen Evolution in PSII

The Cl^- activation of oxygen evolution of PSII can be modeled using the Michaelis-Menten equation.[27] The Michaelis-Menten equation expresses the kinetics of reactions between enzymes and substrates, and it has the form of

$$v = \frac{V_{\max}[s]}{K_m + [s]} \qquad \textbf{Equation 2}$$

Here v is the reaction rate, V_{max} is the maximal reaction rate or the limit of the reaction velocity, K_m is the Michaelis constant or the substrate concentration at which half-maximal rate is achieved, and [s] is the substrate concentration.

Lineweaver and Burk converted this equation to

$$\frac{1}{v} = \frac{K_m}{V_{\max}} \cdot \frac{1}{[s]} + \frac{1}{V_{\max}} \qquad \textbf{Equation 3}$$

The plot of 1/v vs. 1/[s] can be used to find K_m and V_{max} since the line intersects with the 1/[s] axis at $-1/K_m$.[35]

In the presence of inhibitors, the interaction process can be represented as

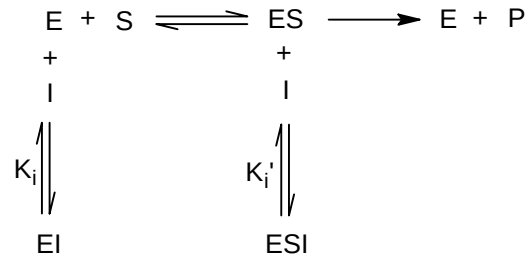

Reaction 7

where E, I, S, P, ES or ESI expresses enzyme, inhibitor, substrate, product, enzyme-substrate complex, or enzyme-substrate-inhibitor complex, respectively. K_i is the dissociation constant of the EI complex (or competitive inhibition constant), and K_i' is the dissociation constant of the ESI complex (or uncompetitive inhibition constant). We have

$$K_i = \frac{[E][I]}{[EI]} \qquad \textbf{Equation 4}$$

$$K_{i'} = \frac{[ES][I]}{[ESI]} \qquad \textbf{Equation 5}$$

When a competitive inhibitor is present, the Michaelis-Menten equation becomes

$$v = \frac{V_{\max}[s]}{K_m\left(1+\frac{[i]}{K_i}\right)+[s]} \qquad \textbf{Equation 6}$$

where [i] is the concentration of inhibitor. Equation 6 can be converted to Equation7.

$$\frac{1}{v} = \frac{K_m}{V_{\max}[s]} + \frac{1}{V_{\max}} + \frac{K_m}{V_{\max}[s]} \cdot \frac{[i]}{K_i} \qquad \textbf{Equation 7}$$

The plot of 1/v vs. [i] is known as the Dixon plot.[35] The intersection point of the straight lines for various [s] values provides a measure of K_i. The Dixon model is useful for competitive inhibition, in which only the EI complex forms, but it does not distinguish between competitive and mixed inhibitors. For mixed or uncompetitive inhibitors, it provides no measure of enzyme-inhibitor-substrate (EIS) complex.[36]

If mixed, uncompetitive and non-competitive inhibitors are also considered, the inhibition kinetic model becomes

$$v = \frac{V_{\max}[s]}{K_m\left[1+\left(\frac{[i]}{K_i}\right)\right]+[s]\left[1+\left(\frac{[i]}{K_i'}\right)\right]} \qquad \textbf{Equation 8}$$

Cornish-Bowden developed an analysis method based on this equation:

$$\frac{[s]}{v} = \frac{K_m}{V_{\max}}\left(1+\frac{[i]}{K_i}\right)+\frac{[s]}{V_{\max}}\left(1+\frac{[i]}{K_i'}\right) \qquad \textbf{Equation 9}$$

A plot of [s]/v vs. [i] is a Cornish-Bowden plot.[36] The intersection point of the straight lines for different [s] values provides a measure of K_i'. The Dixon plots and the

Cornish-Bowden plots for the various inhibition types or modes are shown in Figure 5.

The mathematical models for the effects of ions on oxygen evolution activity of PSII have an important role in the research of oxygen evolution. They have been widely used in the study of the effects of anion activators and inhibitors. Chloride can be treated as a substrate in these models. In these treatments, Cl^- is actually an activator, not a substrate; but the treatment works anyway.

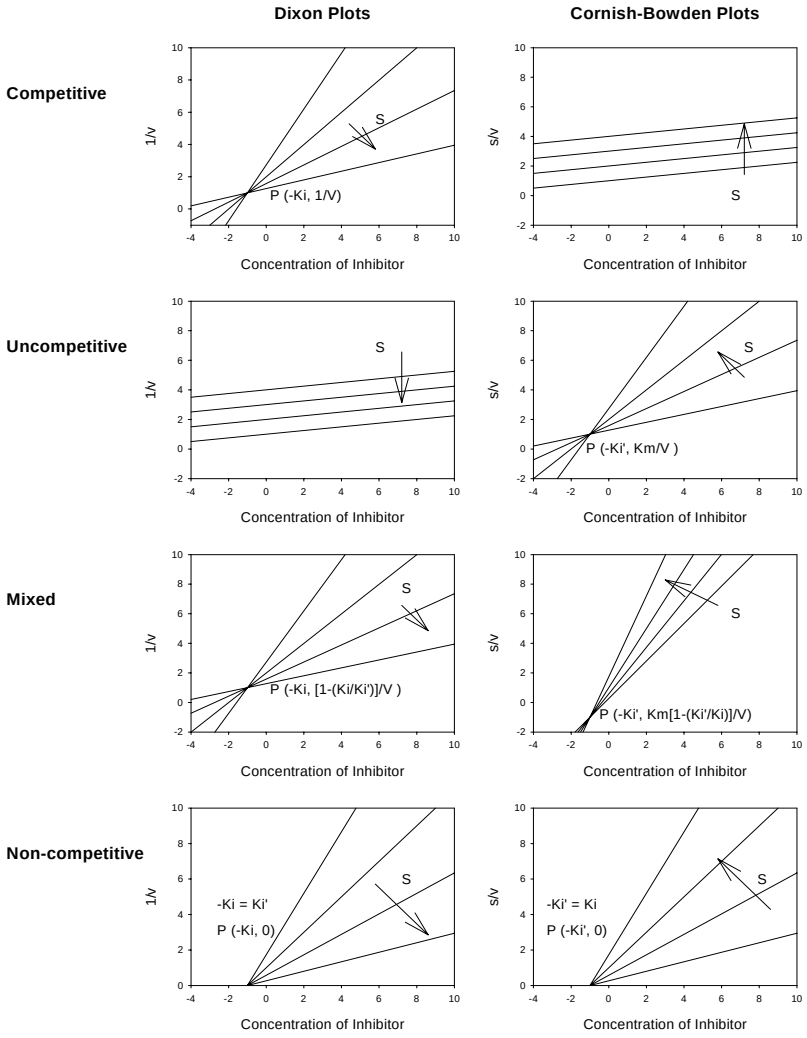

Figure 5 Dixon plots and Cornish-Bowden plots for different inhibition modes [36]

Literature Review

Many studies of the kinetic models of the effects of anions, small molecule effectors and pH in the oxygen evolving process have been done. The studies of the pH dependence of oxygen evolution activity for Cl^- activation began decades ago. In a review article published in 1985, Christa Critchley summarized the research on the pH dependence of oxygen evolution activity with or without added Cl^- in intact Cl^- depleted PSII up until that time.[15] These studies included those of Gorham et al. in 1952, the Izawa et al. in 1969, the Theg et al. in 1982, and the Critchley in 1983. The studies were carried out using Cl^- deficient thylakoid membranes, and showed that the optimal pH was 6.0-7.5 without added Cl^- and the optimal pH was 6.5-8.0 in the presence of added Cl^-.

Early in 1984, Sandusky and Yocum carried out experiments on NH_3 and Tris inhibition of oxygen evolution activity in spinach PSII membranes (they used a PSII preparation.) at various chloride concentrations and presented both Dixon plots and Cornish-Bowden plots of the data.[37] From the plots, K_i and K_i' were found to be 0.22 mM NH_3 and 0.58 mM NH_3 respectively. The two values were close but not equal, which indicated that NH_3 was a mixed competitive inhibitor of Cl^- activation, with one site probably identified with the Cl^- binding site. Therefore, the severity of NH_3

inhibition of photosynthetic oxygen evolution was attenuated in the presence of Cl^-. The higher concentrations of Cl^- resulted in lower inhibition levels.

Later on, Sandusky and Yocum published their research on F^- inhibition of oxygen evolution on PSII in 1986.[38] They studied the effect of F^- at various concentrations of Cl^- and found that F^- was also an inhibitor of oxygen evolution in competition with chloride at pH 7.5. The Dixon and the Cornish-Bowden plots showed that K_i was about 4 mM and K_i' was greater than 60 mM. The K_i' value was 10 fold more than the K_i value which indicated that F^- was a competitive inhibitor of Cl^- in oxygen evolution.

In 1988, Peter Homann published his studies of the pH effects on the Cl^- and Ca^{2+} requirements of photosynthetic water oxidation.[6] First, he investigated the pH dependence of the Cl^- activation of intact Cl^- depleted PSII and 17 and 23 kDa polypeptide-depleted PSII from Phytolacca for the pH range between 4.3 and 7.4. He found that the residual activity was considerably higher at lower pH, and that the concentration of Cl^- had little effect on the oxygen evolution activity for both types of PSII when pH < 5. The Lineweaver-Burke plots (1/v versus 1/[Cl^-]) showed that the oxygen evolution activity was more sensitive to the change of Cl^- concentration at higher pH than at lower pH for PSII both with and without the extrinsic 17 and 23 kDa

polypeptides in the pH range of 5.1-7.4. After that, Homann studied the pH dependence of the activation of the 17 and 23 kDa polypeptide-depleted PSII by Ca^{2+} using *P. americana* and *S. oleracea* PSII membranes, in the presence of 35 mM NaCl. It was evident that O_2 evolution activity reaches its peak value in the pH range of 6.0-7.0. In the case of the 17 and 23 kDa protein-depleted PSII, the overall activity decreased substantially at all pHs. The O_2 evolution activity increased with the addition of $CaCl_2$, but was still below the activity of PSII containing the 17 and 23 kDa subunits. These results indicate that the O_2 evolution activity is reduced after removing the subunits, and that $CaCl_2$ stimulates the activity, which is a typical effect observed for NaCl-washed PSII. The studies also showed that there was no difference in the oxygen evolution activity in intact *P. americana* PSII with or without added $CaCl_2$ (2 mM). The pH value for optimal activity was 6.0-6.5 for intact PSII. The peak pH value for NaCl-washed PSII was 6.5-7.0 in the absence of $CaCl_2$, but shifted back to 6.0-6.5 in the presence of $CaCl_2$. The pH dependence plots for both *P. americana* and *S. oleracea* PSII membranes revealed that the plot shapes at higher pH values (the right side of the peaks) did not change and only those at lower pH values (the left side of the peaks) changed after the extrinsic subunits were removed.

On the other hand, studies related to the effects of NO_2^- of oxygen evolution of PSII were conducted in only a few research groups. In a study on the photosynthetic nitrite reduction by dithioerythritol and the effect of nitrite on electron transport,[39] Spiller and Böger found that, in a medium containing ferricyanide, 72% inhibition of oxygen evolution rates was reached by adding 10 mM NO_2^- in the fragmented chloroplasts isolated from the heterocont alga *Bumilleriopsis filiformis*. They also found that NO_3^- inhibited the oxygen evolution process. The plot of % inhibition vs. log [NO_2^-] gave a straight line with a positive slope, which meant the inhibition increased with the concentration of NO_2^-; the plot of % inhibition vs. log [NO_3^-] gave a concave exponential, which also meant that the inhibition effect enhanced with the concentration of NO_3^-. Moreover, NO_2^- was a much stronger inhibitor, compared to NO_3^-.

In 1985, Stemler and Murphy reported that oxygen evolution rates could be inhibited by 60% in maize chloroplasts in the presence of 20 mM NO_2^-.[40] This investigation further confirmed that NO_2^- inhibited oxygen evolution activity in PSII.

Recently, Sahay et al. reported their studies on the site of action of nitrite inhibition of oxygen evolution in PSII.[19] Using thermoluminescence in spinach thylakoid

membranes under ion-deficient and ion-sufficient conditions, they found that the site of action of NO_2^- was at the side associated with electron donation in PSII, which was unique to NO_2^- inhibition. Other anions tested in their studies, such as formate, fluoride and nitrate, could not replace NO_2^- at the side associated with election donation for producing the same inhibitory effect.

The effects of Br^-, I^-, NO_3^-, F^- and CH_3COO^- on oxygen evolution activity of Cl^- depleted PSII were studied by Hasegawa and coworkers who used FTIR spectroscopy.[41] Their results revealed that the overall features of spectra from Br^-, I^-, and NO_3^- substituted PSII were similar to those of Cl^-, which confirmed their ability to support oxygen evolution. However, the spectra of F^- and CH_3COO^- substituted PSII were rather different, which was related to the suppression of oxygen evolution by these ions. They also investigated the dependence of oxygen evolution rates on the concentrations of all the anions under saturating and limiting light conditions. The dependence plots showed that under either light condition Br^- and NO_3^- had activating effects similar to Cl^-, and that their activating ability had the order of $Cl^- > Br^- > NO_3^-$. Meanwhile, I^- behaved like an activator at low concentrations and an inhibitor at higher concentrations; F^- and CH_3COO^- were only inhibitory, and their inhibiting effects were very close

with CH_3COO^- slightly stronger under the limiting light conditions. In general, the activity in the presence of all related anions under saturating light was much higher than those under limiting light (over 7 fold higher in the case of Cl^-).

CHAPTER III

MATERIALS AND METHODS

This thesis focuses mainly on analysis of complex enzyme kinetic data that were collected by previous students in the Haddy laboratory. Therefore, only a few of the experiments presented were performed by the author. T. Delaney Santoro performed the experiments on the pH dependence of oxygen evolution under F^- inhibition in intact PSII, based on the method of Thomas Kuntzleman. Madhu Kumar collected all of the data from the experiments on NO_2^- inhibition in the presence of Cl^-. The author completed the experiments on NO_2^-, NO_3^- and Cl^- dependence of oxygen evolution in intact Cl^- depleted PSII and NaCl-washed PSII. The intact Cl^- depleted PSII membranes were prepared by Xiaoming Li. The NaCl-washed PSII was prepared by Alice Haddy and the author, using intact PSII membranes provided by Alice Haddy.

I. The Methods for Experiments

Preparation of Intact PSII

The original preparation method of intact PSII-enriched thylakoid membranes was described by Berthold and coworkers in 1981.[33] The preparation used here was modified from the original by others a few years later.[16, 42] The PSII

was generally prepared by other members of the laboratory and stored as pellets at about 10 milligrams of chlorophyll per mL (mg Chl/mL) in Buffer I (0.4 M sucrose, 20 mM MES and 15 mM NaCl, pH = 6.3, adjusted with NaOH) in liquid nitrogen.

Preparation of NaCl-washed PSII

NaCl-washed PSII-enriched membranes were prepared from intact PSII, by a method similar to that reported by Miyao and Murata in 1983.[34] It was slightly changed by the author's research advisor Alice Haddy, and consists of the following procedure.

About 5-10 mg Chl of intact PSII was suspended into 30 mL of Buffer III (0.4 M sucrose, 20 mM MES, and 1.5 M NaCl, pH = 6.3, adjusted with NaOH) using a small brush. The mixture was incubated on ice for 30-60 minutes, and then centrifuged at 13 K rpm in a Beckman JA 20 rotor for 8 minutes. The pellets were resuspended in 30 mL of Buffer II (0.4 M sucrose and 20 mM MES, pH = 6.3, adjusted by using NaOH) and the mixture centrifuged 8 minutes at 13 K rpm in a Beckman JA 20 rotor. This step was repeated twice. After resuspending the NaCl-washed PSII to about 1.5 mg Chl/mL in Buffer II, it was stored as 1.5 mL aliquots in liquid nitrogen for future use.

Chloride Depletion Method of Intact PSII

Removal of Cl^- from intact PSII was carried out by dialysis, which was conducted by Xiaoming Li as described in his thesis.[5] This technology was based on the method presented by Lindberg et al.,[28] and modified by pretreating the intact PSII with Br^-.

Determination of Chlorophyll Concentration

Before measuring oxygen evolution rates, the concentration of chlorophyll was determined according to the method of Arnon (1949).[43] A PSII suspension was diluted using a solution of 80% (v/v) acetone and 20% (v/v) demineralized water. The diluted mixture was centrifuged to remove the starch as a pellet. The absorbance was measured at 645 nm and 663 nm using a UV-Vis spectrophotometer (Shimazu UV-1201). Three duplicate measurements were averaged.

The chlorophyll concentration of the diluted mixture was calculated by using the following equations.[43] For chlorophyll a and chlorophyll b in mg/L, we have

$$C_a = -2.69A_{645} + 12.7A_{663} \qquad \textbf{Equation 10}$$

$$C_b = 22.9A_{645} - 4.68A_{663} \qquad \textbf{Equation 11}$$

$$C_{total} = 20.2A_{645} + 8.0A_{663} \qquad \textbf{Equation 12}$$

where C_a, C_b and C_{total} are the concentrations of chlorophyll a, chlorophyll b, and all chlorophylls, and A_{645} and A_{663} are the absorbance values at 645 nm and 663 nm, respectively. The actual concentration of chlorophyll in the PSII suspension was determined by considering the dilution factor from dissolving in the 80% acetone solution.

Assay of Oxygen Evolution Activity

Oxygen evolution activity was measured using a Clark-type O_2 selective electrode (Yellow Spring Instruments model 5331) equipped with a temperature-controlled water bath, a glass-jacketed reaction cell, a signal processor, saturating light sources, a stirrer, and a computer with data collection software programmed by Sergei Baranov. The temperature of the water bath, the reaction cell, and assay buffers was kept at 25°C during the assays.

The PSII sample to be measured was chilled on ice. The oxygen electrode was calibrated using demineralized water and water saturated with O_2 (about 260 µM O_2). Before the assay, the buffer was purged with N_2 gas to remove O_2. The PSII sample was incubated with the buffer in the reaction cell for 2 minutes before the light sources were turned on. As electron acceptor, 1 mM phenyl-p-benzoquenone (PPBQ) was added from a 50 mM stock solution in dimethyl sulfoxide. The maximum slope of voltage due to O_2 reduction at the

electrode versus time was taken, and using the relevant input parameters, the oxygen evolution rate was calculated by the program. All of the given rates represent the averages of three or more measurements.

The assay buffers contained the specified concentrations of F^-, NO_2^-, NO_3^- or Cl^-. They were prepared by adding NaF, $NaNO_2$, $NaNO_3$ or NaCl from stock solutions to Buffer II or Buffer IV (0.4 M sucrose and 20 mM MES, pH = 6.3, adjusted with $Ca(OH)_2$), depending on the application. The assay buffers for the experiments of NO_2^-, NO_3^- and Cl^- dependence of oxygen evolution were prepared by the author, and the rest of the assay buffers were prepared by other students during their own experiments.

pH Dependence of O_2 Evolution under Fluoride Inhibition in Intact PSII

The pH dependence data were collected by T. Delaney Santoro according to the experimental method presented by Thomas Kuntzleman.[44] A series of buffers from pH 4 to pH 8 was made using glutaric acid (pH 4.01-4.61), malic acid (pH 4.81-5.41), itaconic acid (pH 5.15-5.75), MES (pH 5.79-6.39), PIPES (pH 6.46-7.06), MOPS (pH 6.90-7.50), and HEPES (pH 7.20-7.80). Each buffer solution contained 20 mM buffer, 1.0 mM NaCl, 0.4 M sucrose, and the specified amount of NaF. A control measurement in 0.4 M sucrose, 20

mM MES, 1.0 mM NaCl, and 30 mM NaF (pH = 6.3) was used to normalize the measurements from the various pHs.

II. Data Analysis Methods

Tools for Mathematical Modeling

Sigma Plot 8.0 was used as a tool for mathematical modeling. This software is a state-of-the-art technical graphing program designed for the Windows platform.[45] After the data for oxygen evolution rates were averaged or converted to the data for Dixon plots and Cornish-Bowden plots, they were input into the worksheets. Then the equations used to fit the data were set up as subroutines based on the related equilibria among enzymes, substrates, inhibitors, and their combinations. The initial parameters were set and the data fitted to the equation using a nonlinear least squares routine, giving optimized values for the dissociation constants. The fitted curves were plotted on the graphs along with the original data.[46]

Mathcad 2000 was used as a tool to assist in the data treatment and analysis, to complement the Sigma Plot calculations.

Calculation of the pH Dependence of Oxygen Evolution Activity under F^- Inhibition

For each pH dependence curve, the oxygen evolution activity was initially modeled using Equation 1 to find apparent dissociation constants in the presence of varying amounts of F^-. This analysis provided a starting point before extending the model to more complex equilibria.

$$A = \frac{A_{max}}{1 + \frac{[H^+]}{K_1} + \frac{K_2}{[H^+]}} \qquad \textbf{Equation 1}$$

where K_1 is the apparent proton dissociation constant for an acidic residue, K_2 is the apparent proton dissociation constant for a basic residue, A_{max} is the theoretical maximum activity as the acidic residue is deprotonated and the basic residue is protonated optimally. The pH dependence curve in the absence of F^- was taken to represent true values of K_1 and K_2, the protonation and deprotonation constants of the residues that determine the uninhibited pH dependence.

For the pH dependence of oxygen evolution under F^- inhibition, two models were used to account for the effect of the inhibitor. The simpler model assumed binding of F^- to two protonation states of PSII. This simplified model can be expressed as

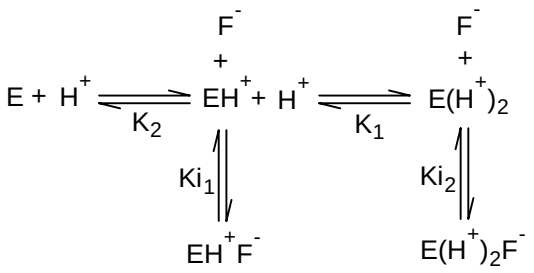

Reaction 8

and the pH dependence equation from the above scheme is

$$A = \frac{A_{\max}}{1 + \frac{[H]}{K_1} + \frac{K_2}{[H]} + [F]\left(\frac{1}{K_{i1}} + \frac{[H]}{K_1 K_{i2}}\right)}$$

Equation 13

Here [F] is the concentration of F^-. K_{i1} and K_{i2} are the dissociation constants of fluoride inhibition for EH^+F^- and $E(H^+)_2F^-$ respectively.

The modeling process was carried out in two stages. (1) A_{max}, K_1 and K_2 were found first, by fitting the data of 0 mM F^- (the sample without F^-) using Sigma Plot. Using the values of A_{max}, K_1 and K_2, the values of K_{i1} and K_{i2} were determined by separately fitting the data for 5, 10, 15 and 20 mM of F^-. The values obtained for K_{i1} or K_{i2} are expected to be the same for all concentrations of F^-, but actually they were somewhat different for various concentrations of F^-. (2) Using the value obtained for A_{max} as a constant, and using the obtained values of K_1 and K_2 and the selected values of K_{i1} and K_{i2} from Step (1) as initial guesses for parameters, the curve fitting was carried out for all F^-

concentrations in one regression. The best values of K_1, K_2, K_{i1} and K_{i2} for all curves were reached through adjusting the parameters within the Sigma Plot program. Along with A_{max}, these best K values were the constants for the simplified model.

For the comprehensive model, F^- was assumed to bind to three protonation states of PSII. In this case the reaction scheme is

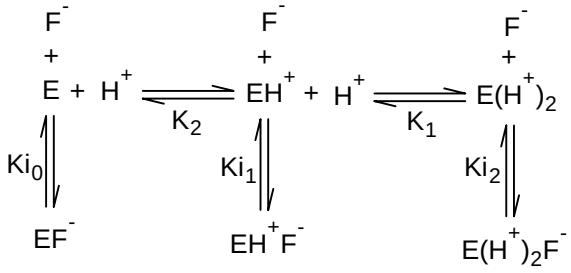

Reaction 9

and the pH dependence equation is

$$A = \frac{A_{\max}}{1 + \frac{[H]}{K_1} + \frac{K_2}{[H]} + [F]\left(\frac{1}{K_{i1}} + \frac{[H]}{K_1 K_{i2}} + \frac{K_2}{K_{i0}[H]}\right)}$$

Equation 14

which now includes K_{i0}, the dissociation constant for EF^-. As in the simplified model, the values for A_{max}, K_1 and K_2 were determined from the 0 mM F^- data, followed by the determination of the dissociation constants for inhibition (K_{i0}, K_{i1}, and K_{i2}) for each concentration of F^-. Then, using A_{max} as a constant and the obtained K_1, K_2, K_{i0}, K_{i1} and K_{i2}

values as initial guesses for parameters, all Ks were fitted in one regression by adjusting the parameters. Eventually, a single set of constants was found using the same method as described above. The set of constants fits all fluoride concentrations simultaneously.

Kinetic Models of NO_2^- or NO_3^- Dependence of O_2 Evolution in PSII

After removal of the 17 and 23 kDa subunits, PSII is expected to have no O_2 evolving activity in the absence of added activating anions such as Cl^-. However, the NaCl-washed PSII may still contain very small amount of residual Cl^- even though it has been washed in Cl^- free buffer. Meanwhile, NO_2^- or NO_3^- has both activating and inhibiting effects, so the expression (Equation15) for the NO_2^- or NO_3^- dependence of O_2 evolution rate in NaCl-washed PSII consists of two parts: the first part is based on a substrate inhibition model including activation as well as inhibition, and the second is a constant, V_0, that accounts for the low residual activity.[4] The substrate inhibition model can be expressed by the scheme of Reaction 10, in which E and S are enzyme and substrate respectively.

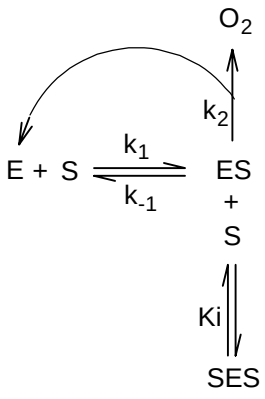

Reaction 10

$$v = \frac{V_{\max}[s]}{K_m + [s] + \frac{[s]^2}{K_i}} + V_0 \qquad \textbf{Equation 15}$$

In Equation15, K_m is the Michaelis constant for activation, [s] is the concentration of substrate (NO_2^- or NO_3^- here), K_i is the dissociation constant for inhibition, V_{max} is the maximum reaction velocity, and V_0 is the residual activity at 0 mM NO_2^- or NO_3^-.

For each experiment, the control experiment for activation of oxygen evolution by chloride was performed. Chloride activation of O_2 evolution is well known, and follows the Michaelis-Menten equation, Equation 16, including the residual activity that is probably due to bound Cl^-.[5]

$$v = \frac{V_{\max}[s]}{K_m + [s]} + V_0 \qquad \textbf{Equation 16}$$

where [s] is the concentration of substrate, which is chloride here. The values of K_m, V_{max}, and K_i in Equations 15 and 16 were found using the Sigma Plot program, by curve fitting of the experimental data points. Equation 16 is Equation 2 with the addition of V_0.

In the case of intact PSII, the model is essentially the same model as that for NaCl-washed PSII except that there is a high amount of residual activity at zero added anion. The high residual activity is because PSII dialyzed against a Cl^- free buffer to remove bound Cl^- loses only about 65% of the control activity.[27] Moreover, the Cl^- depletion was done by Br^- pretreatment, so residual activity may be due to bound Cl^- or Br^-. Equation 17 below is for the NO_2^- or NO_3^- dependence of O_2 evolution in intact Cl^- depleted PSII. It is similar to Equation15, except that the residual activity is also subject to inhibition.[4]

$$v = \frac{V_{\max}[s]}{K_m + [s] + \frac{[s]^2}{K_i}} + \frac{V_0}{1 + \frac{[s]}{K_i}} \qquad \textbf{Equation 17}$$

The control experiments to measure Cl^- activation were also carried out using intact Cl^- depleted PSII. The exact constant values were determined as for NaCl-washed PSII.

CHAPTER IV

RESULTS

I. Mathematical Models for pH Dependence of Oxygen Evolution Rates under F^- Inhibition in Intact PSII

pH Dependence under F^- Inhibition of Oxygen Evolution in Intact PSII

In previous experiments carried out in the Haddy lab, T. Delaney Santoro investigated the pH dependence of F^- inhibition of O_2 evolution in intact PSII in the presence of 1 mM NaCl. The data showed a clear changing pattern of O_2 evolving activity vs. pH under the various concentrations of F^- (Figure 6), and they represent a complex equilibrium between PSII, F^-, and H^+. The maximum in the O_2 evolution activities shifted to higher pH while the overall activity decreased. The peak values were about 110%, 90%, 80%, 75%, and 65% activity for 0 mM, 5 mM, 10 mM, 15 mM, and 20 mM F^- concentrations respectively, corresponding to the optimal pHs of 6.2, 6.3, 6.4, 6.5, and 6.6.

To approach the problem, the data were analyzed using increasing levels of complexity. The equations of the kinetic models for the pH dependence of F^- inhibition of O_2 evolution in intact PSII were derived according to the related reaction schemes shown as follows. First, the individual curves were fit to a model assuming two protonation events (Reaction 6), as given in Equation 1.

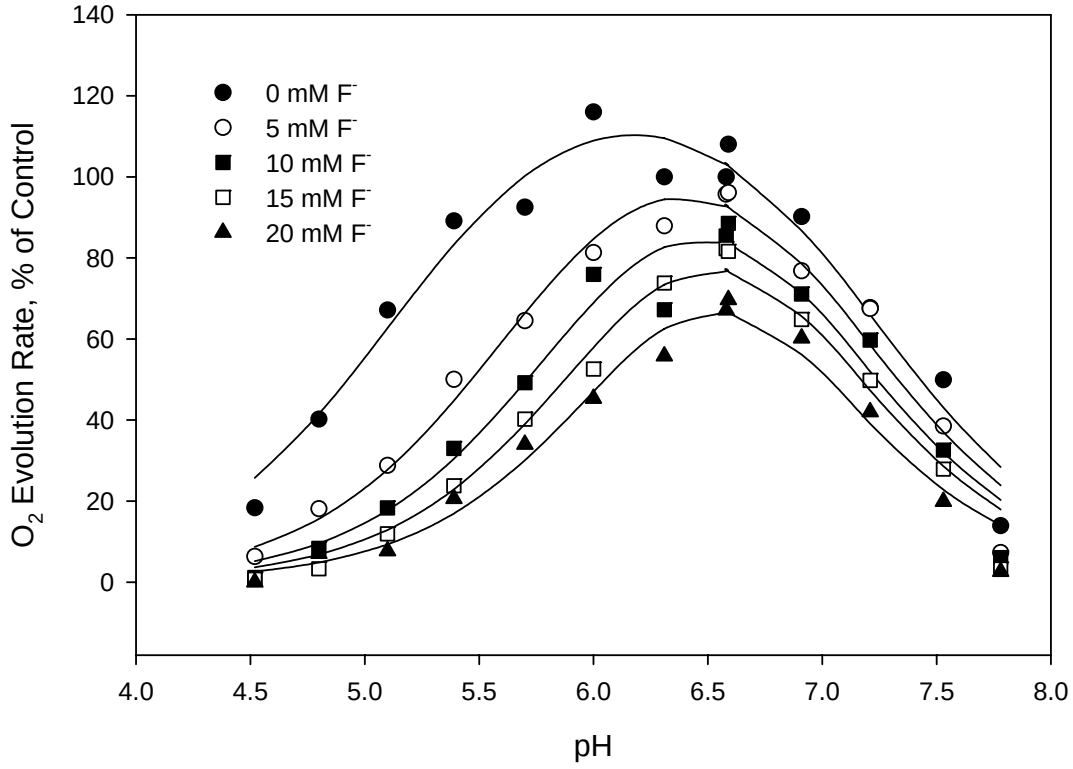

Figure 6 pH dependence of O_2 evolution rate in intact PSII under F^- inhibition. The data were collected by T. Delaney Santoro, and 1 mM Cl^- was present in each sample. The curves represent fits assuming only 2 acid dissociation events.

This model assumes that EH^+ is the active species. By analyzing the data using Sigma Plot, the values of A_{max}, K_1 and K_2 for 0 mM F^- were found to be 130%, 7.5×10^{-6} M and 6.0×10^{-8} M, where A_{max} is the maximum activity or the activity when all E related species are in the form of EH^+. The y-scale for the figure is expressed in percentage, where 100% was set to an observed rate at pH 6.3 and the value was used as a reference. Using A_{max} = 130% as a constant and fitting to Equation 1, the pK_1 and pK_2 values for 5, 10, 15 and 20 mM fluoride concentrations were obtained using Sigma Plot in separate fits (Table 1). In Table 1, the values of pK_1 and pK_2 are those of the acidic dissociation constant pK_a and the basic dissociation constant pK_a.

Table 1 Apparent acid dissociation constants for the pH dependence of O_2 evolution rates in various F^- concentrations

Constant	0 mM F^-	5 mM F^-	10 mM F^-	15 mM F^-	20 mM F^-
pK_1	5.12±0.053	5.66±0.047	5.89±0.057	6.06±0.046	6.21±0.046
pK_2	7.23±0.056	7.13±0.051	7.05±0.058	7.00±0.048	6.85±0.047

The acidic pK_a (or pK_1) increased and the basic pK_a (or pK_2) decreased with increasing F^- concentration. Because these pK_a values are only apparent values, further analysis

was undertaken to determine inherent dissociation constants for F^- binding.

A Simplified Model of the pH Dependence of O_2 Evolution under F^- Inhibition

Based on the above analysis, a kinetic model was built. This model includes equilibria for both protonation and F^- binding to two forms of the enzyme, EH^+ and $E(H^+)_2$, as shown in Reaction 8. EH^+ is still assumed to be the active species, while all other forms of the enzyme are inactive. Although F^- is a competitive inhibitor of Cl^-, the equilibrium with Cl^- is not shown and sufficient Cl^- is assumed to be present.

In the scheme of Reaction 8, EH^+ complex was again assumed to be the active center that can give product (O_2). The mathematical expression is given in Equation13. The model presented by Reaction 8 and Equation 13 is a simplified model since the binding of F^- and E is not included. The reason for this was to limit the number of parameters that must be fitted. It can be seen that the greater effect of F^- was on the protonated forms, and thus we simplified the modeling process.

During the curve-fitting process using Sigma Plot, three steps were carried out: (1) A_{max}, K_1 and K_2 were determined with the data for 0 mM F^-; (2) A_{max}, K_1 and K_2 were used as constants to find K_{i1} and K_{i2} for 5, 10, 15 and 20 mM F^- in

separate fits, but these K_{i1} and K_{i2} were somewhat different for the different F^- concentrations; (3) As parameters, K_1, K_2, K_{i1} and K_{i2} were fitted for all F^- concentrations in one step. During the fitting process, the A_{max} value obtained in Step (1) was used as a constant, the K_1 and K_2 values obtained in Step (1) were used as initial parameters for K_1 and K_2, one of the K_{i1} values obtained in Step (2) was selected as the initial parameters for K_{i1}, and the same method was used to select the initial parameter for K_{i2}. After the initial parameters were input into the Sigma Plot routine, the fitted parameters of K_1, K_2, K_{i1} and K_{i2} were found by adjusting the initial parameters to make R^2 optimal. This resulted in one unique value for each of K_1, K_2, K_{i1} and K_{i2}, which fit all concentrations of F^- and represented the simplified model. Generally, the existence of F^- would not impact the protonation and deprotonation equilibria. Therefore, A_{max}, K_1 and K_2 would be unchanged with the concentration of F^-.

After fitting the data for 0 mM F^-, it was found that $A_{max,}$ K_1, and K_2 were 130%, 7.5×10^{-6} M, and 6.0×10^{-8} M, and certainly, the values were the same as in the last section. In the next step, K_{i1} and K_{i2} for 5, 10, 15 and 20 mM F^- were determined separately. The values are listed in Table 2, where K_{i1} and K_{i2} are slightly different for the different concentrations of fluoride and range from 33-61 mM for K_{i1}

and 2.3-2.7 mM for K_{i2}. It must be mentioned that K_{i1} or K_{i2} should have only one value for each and does not change with fluoride concentration. The individual fits were designed to find a reasonable value range for K_{i1} or K_{i2} respectively. This made the modeling process easier. The plots of activity vs. pH are given in Figure 7 through Figure 11.

Table 2 K_{i1} and K_{i2} of the simplified model for different F^- concentrations by individually curve-fitting

Inhibition Constant	5 mM F^-	10 mM F^-	15 mM F^-	20 mM F^-
K_{i1} (mM)	61 ± 45	50 ± 26	60 ± 32	33 ± 11
K_{i2} (mM)	2.3 ± 0.5	2.5 ± 0.7	2.4 ± 0.7	2.7 ± 1.0

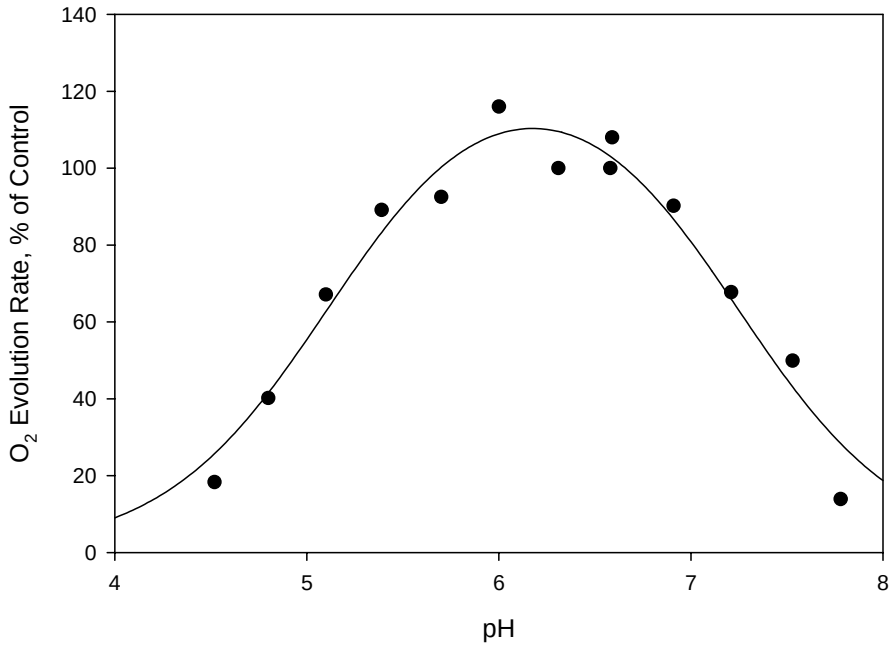

Figure 7 Individual fitted plot of the simplified model for pH dependence of O_2 evolution of PSII for 0 mM F^-. The data were collected by T. Delaney Santoro, and 1 mM Cl^- was present in each sample. A_{max}, K_1 and K_2 were fitted here. A_{max} = 130%, $K_1 = 7.5\times10^{-6}$ M, and $K_2 = 6.0\times10^{-8}$ M.

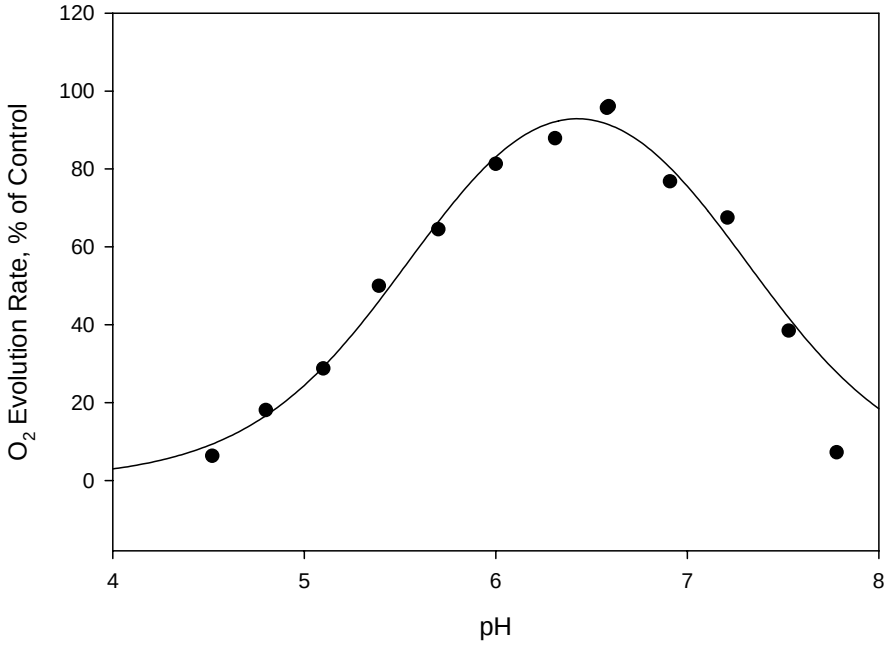

Figure 8 Individual fitted plot of the simplified model for pH dependence of O_2 evolution of PSII for 5 mM F^-. The data were collected by T. Delaney Santoro, and 1 mM Cl^- was present in each sample. A_{max}, K_1 and K_2 were set, and K_{i1} and K_{i2} were fitted here. A_{max} = 130%, $K_1 = 7.5\times10^{-6}$ M, and $K_2 = 6.0\times10^{-8}$ M. K_{i1} and K_{i2} are shown in Table 2.

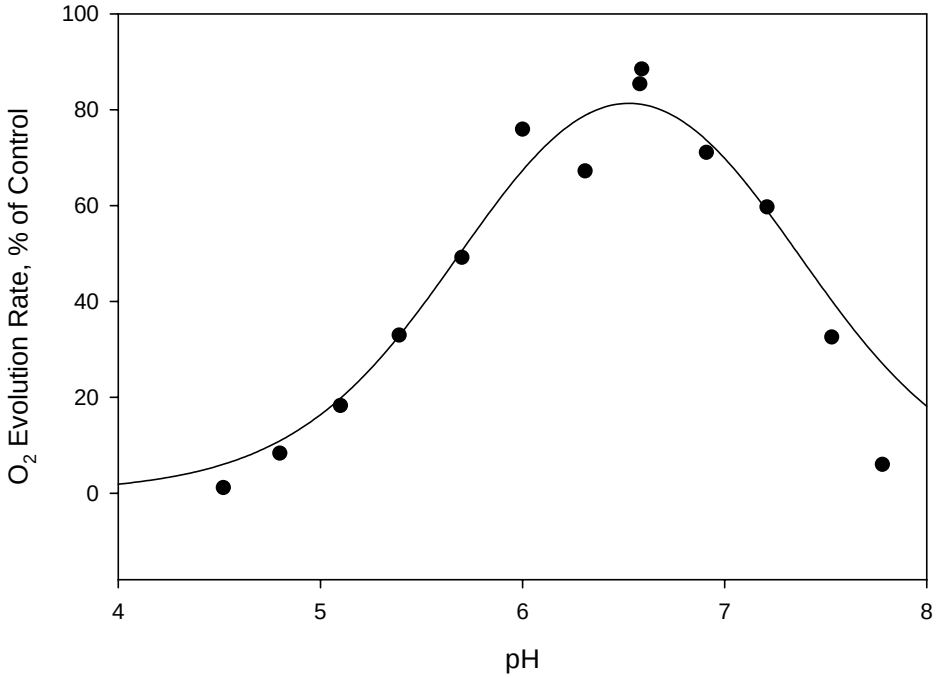

Figure 9 Individual fitted plot of the simplified model for pH dependence of O_2 evolution of PSII for 10 mM F^-. The data were collected by T. Delaney Santoro, and 1 mM Cl^- was present in each sample. A_{max}, K_1 and K_2 were set, and K_{i1} and K_{i2} were fitted here. A_{max} = 130%, $K_1 = 7.5\times10^{-6}$ M, and $K_2 = 6.0\times10^{-8}$ M. K_{i1} and K_{i2} are shown in Table 2.

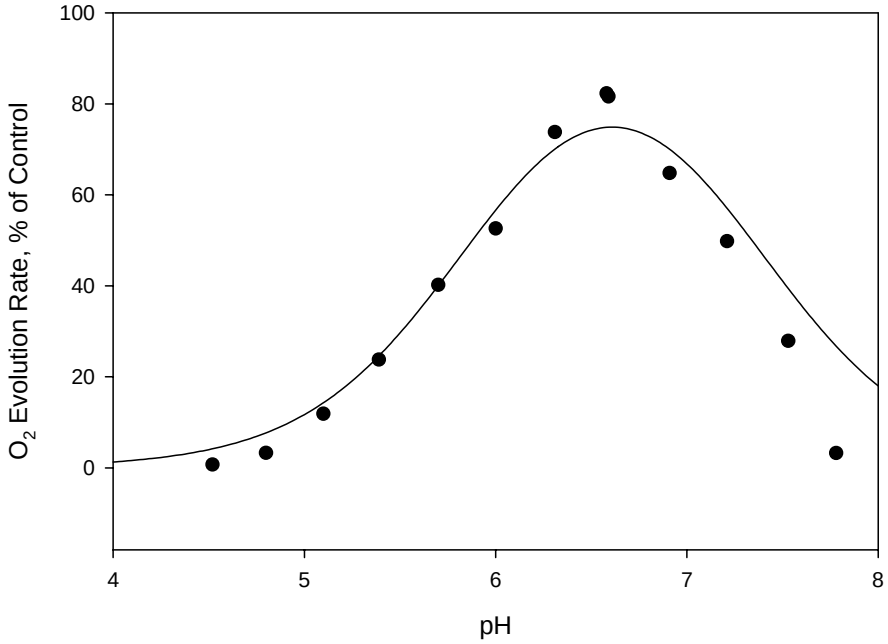

Figure 10 Individual fitted plot of the simplified model for pH dependence of O_2 evolution of PSII for 15 mM F^-. The data were collected by T. Delaney Santoro, and 1 mM Cl^- was present in each sample. A_{max}, K_1 and K_2 were set, and K_{i1} and K_{i2} were fitted here. A_{max} = 130%, $K_1 = 7.5\times10^{-6}$ M, and $K_2 = 6.0\times10^{-8}$ M. K_{i1} and K_{i2} are shown in Table 2.

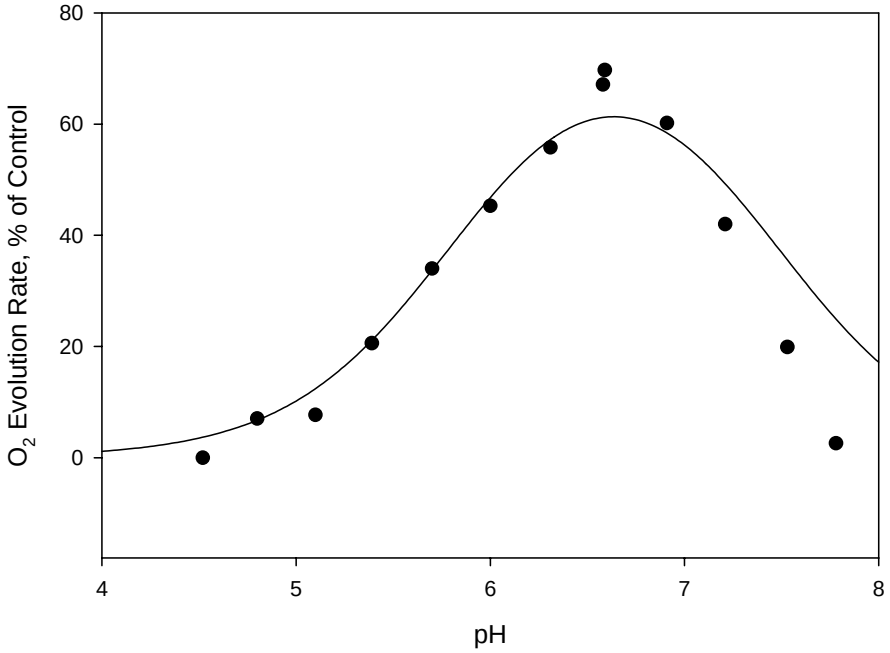

Figure 11 Individual fitted plot of the simplified model for pH dependence of O_2 evolution of PSII for 20 mM F^-. The data were collected by T. Delaney Santoro, and 1 mM Cl^- was present in each sample. A_{max}, K_1 and K_2 were set, and K_{i1} and K_{i2} were fitted here. A_{max} = 130%, $K_1 = 7.5\times10^{-6}$ M, and $K_2 = 6.0\times10^{-8}$ M. K_{i1} and K_{i2} are shown in Table 2.

A single set of values for K_1, K_2, K_{i1} and K_{i2} was found by combining the data for all F^- concentrations into one regression analysis using the Sigma Plot program. Again, the value for A_{max} was set to 130%, but all four equilibria were allowed to vary. This represents the final fit to the simplified model, with equilibria as in Reaction 8 and kinetic equation as in Equation 13. All parameter values and their standard errors are presented in Table 3. R^2 for the regression or the curve fitting equals 0.9509, where R is correlation coefficient. The plots of the final simplified model are given in Figure 12.

Table 3 Equilibrium constants and their standard errors of the final simplified model found from a simultaneous fit of all curves

Constant	Value	Standard Error
pK_1	5.11	0.053
pK_2	7.12	0.036
K_{i1} (mM)	78	30
K_{i2} (mM)	2.2	0.4

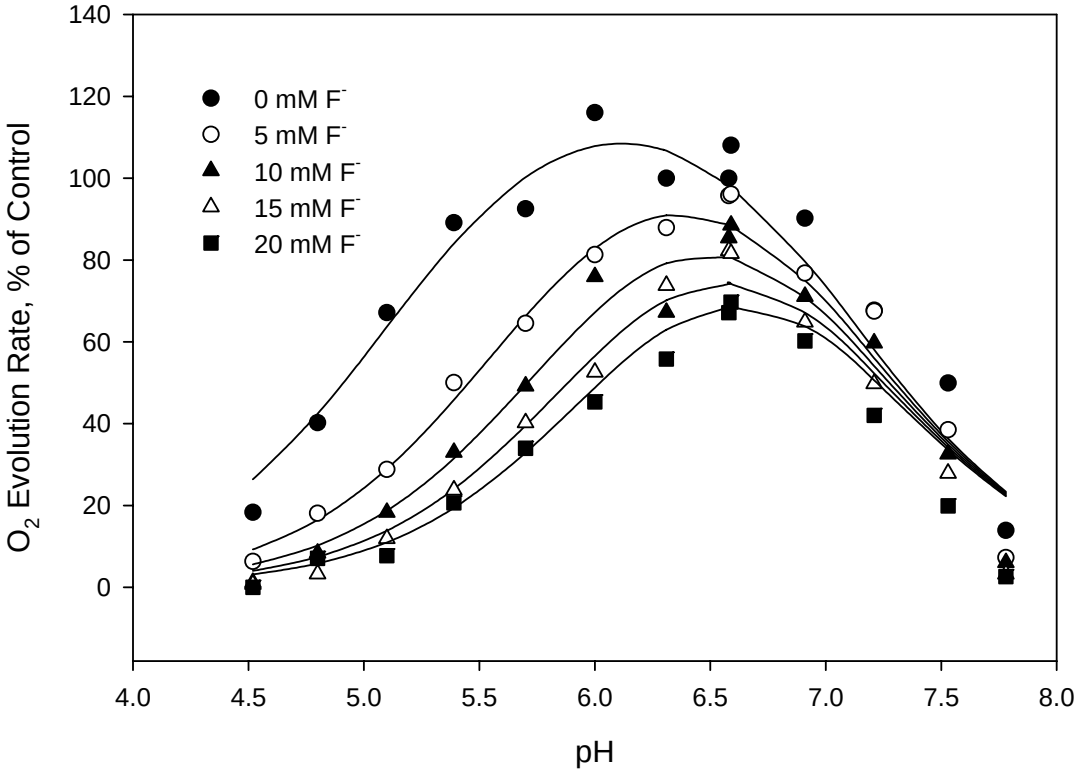

Figure 12 Plots for the simplified model of pH dependence of O_2 evolution rate under F^- inhibition in intact PSII. The data were collected by T. Delaney Santoro, and 1 mM Cl^- was present in each sample. All curves were fitted simultaneously with A_{max} set and K_1, K_2, K_{i1} and K_{i2} allowed to vary. Refer to Table 3 for the values found.

Two interrelated observations about this model were revealed. First, the model did not include the equilibrium for the binding of F^- and OEC (E). Therefore, the model did not fit the experimental data well at the higher pH. A more complex model, which includes the equilibrium for the binding between F^- and E, was then developed.

A Comprehensive Model of the pH Dependence of O_2 Evolution under F^- Inhibition

The more complex (or the comprehensive) model included three equilibria for F^- binding to E, EH^+ and $E(H^+)_2$. Therefore, three parameters (K_{i0}, K_{i1} and K_{i2}) had to be fit at once, which was more difficult. The key to successfully fitting the data to the comprehensive model mainly depends on the method to find all dissociation constants for all related equilibriums in one regression using Sigma Plot program. Like the simplified model, EH^+ was treated as the only active center. From the equilibrium scheme of the comprehensive model (see Reaction 9), the kinetic equation was derived as shown in the Appendix A. The equation is similar to that of the simplified model, but with an additional term involving the inhibition dissociation constant for the EF^- complex, K_{i0} (Equation 14).

All dissociation constants were fitted in one regression using Equation 14 on the Sigma Plot program. A_{max} was set to

130%, as in the simplified model. Setting [F] = 0 mM, K_1 and K_2 were found to be 7.5×10^{-6} M and 6.0×10^{-8} M. These two values were used as initial parameters for K_1 and K_2. K_{i1} (7.8×10^{-2} M) and K_{i2} (2.2×10^{-3} M) from the combined simplified model were used as the initial parameters for K_{i1} and K_{i2}. The initial parameter for K_{i0} was guessed to be 1.5×10^{-2} M. By adjusting the initial parameters for K_1, K_2, K_{i0}, K_{i1} and K_{i2} as well as the tolerance and the step size on the Sigma Plot program, the highest possible R^2 (0.9647) for the regression and the lowest possible standard errors for K_1, K_2, K_{i0}, K_{i1} and K_{i2} were reached. The results for the fit are shown in Table 4 and Figure 13.

Table 4 Determined constants and their standard errors for the comprehensive model from a simultaneous fit of all curves

Dissociation Constant	Value	Standard Error
pK_1	5.13	0.045
pK_2	7.24	0.043
K_{i0} (mM)	15.8	5.3
K_{i1} (mM)	381	183
K_{i2} (mM)	2.0	0.3

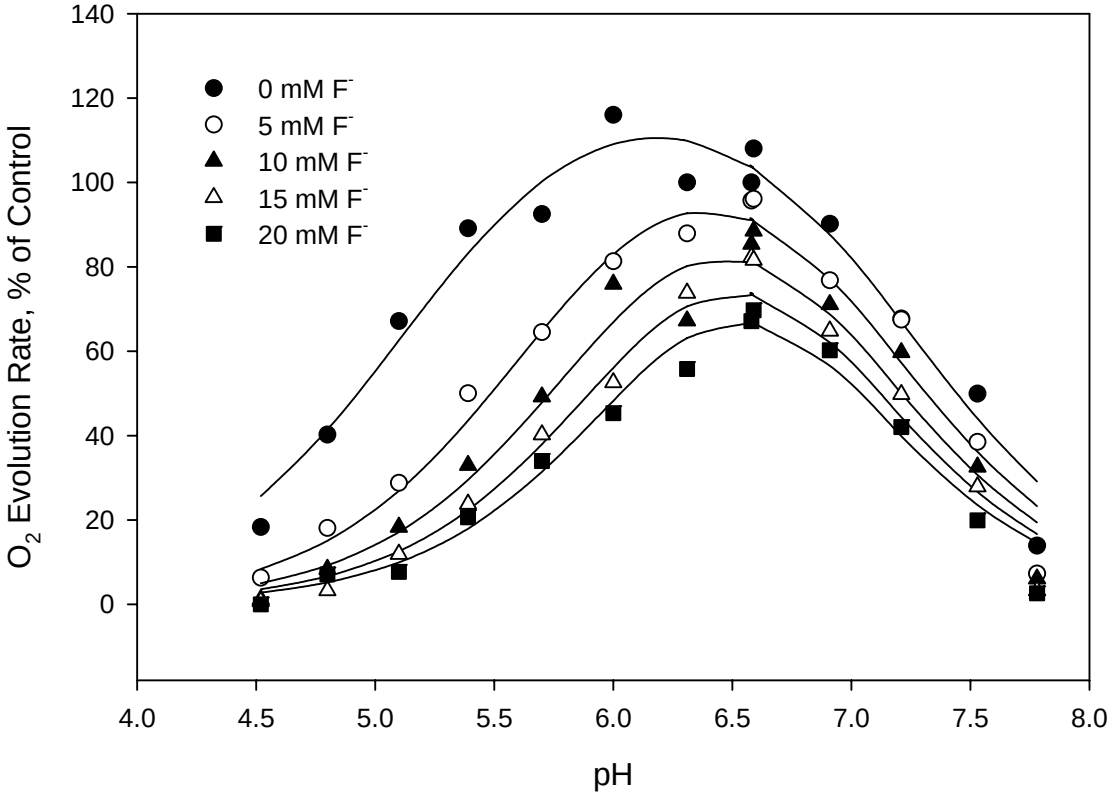

Figure 13 Plots of the comprehensive model for pH dependence of O_2 evolution in intact PSII under F^- inhibition. The data were collected by T. Delaney Santoro, and 1 mM Cl^- was present in each sample. All curves were fitted simultaneously with A_{max} set and K_1, K_2, K_{i0}, K_{i1} and K_{i2} allowed to vary. Refer to Table 4 for the values found.

In summary, the comprehensive model is much better than the simplified model, especially on the higher pH side. This can be seen by comparing Figure 13 with Figure 12, and indicates that the comprehensive model predicts the experimental data quite well.

II. Nitrite Dependence of O_2 Evolution in Intact and NaCl-washed PSII

Nitrite Mode of Inhibition of O_2 Evolution

Some studies on nitrite (NO_2^-) inhibition of oxygen evolution activity in intact and NaCl-washed PSII were carried out previously in the Haddy lab by M. Kumar in 2001 (unpublished). The author analyzed the data from those experiments and found the competitive inhibition constant, K_i, and the uncompetitive inhibition constant, K_i', for NO_2^- for each PSII preparation.

Figure 14 and Figure 15 present the Cornish-Bowden and the Dixon plots of the NO_2^- inhibition in intact PSII and corresponding fits. The fitting routine forced the lines to pass through a common point for each case. The intersection points on the Cornish-Bowden plot and the Dixon plot are at (-13.70, 0.000) and (-28.76, -0.001761), respectively. This means that K_i and K_i' for intact PSII were about 29 mM and 14 mM, respectively. In addition, Figures 16 and 17 present the Cornish-Bowden and the Dixon plots of the NO_2^- inhibition of oxygen evolution in NaCl-washed PSII.

Intersection points at (-0.5863, 0.008404) and (-11.66, -0.03557) indicate that K_i and K_i' for NaCl-washed PSII were about 12 mM and 0.6 mM, respectively. The K_i and K_i' values including their standard errors are given in Table 5. It can be seen from the table that the standard errors of the competitive constant K_i for both types of PSII are very high. This means that values are essentially undetermined. Examination of the plots reveals that the lines in the Dixon plots for both types of PSII are not well separated and could easily be parallel. Hence the K_is are probably actually very large, so there is very little competitive inhibition.

Table 5 K_i and K_i' values and their standard errors of NO_2^- inhibition

	K_i (mM)	K_i' (mM)	Standard error of K_i	Standard error of K_i'
Intact PSII	29	14	243	12
NaCl-washed PSII	12	0.60	247	0.72

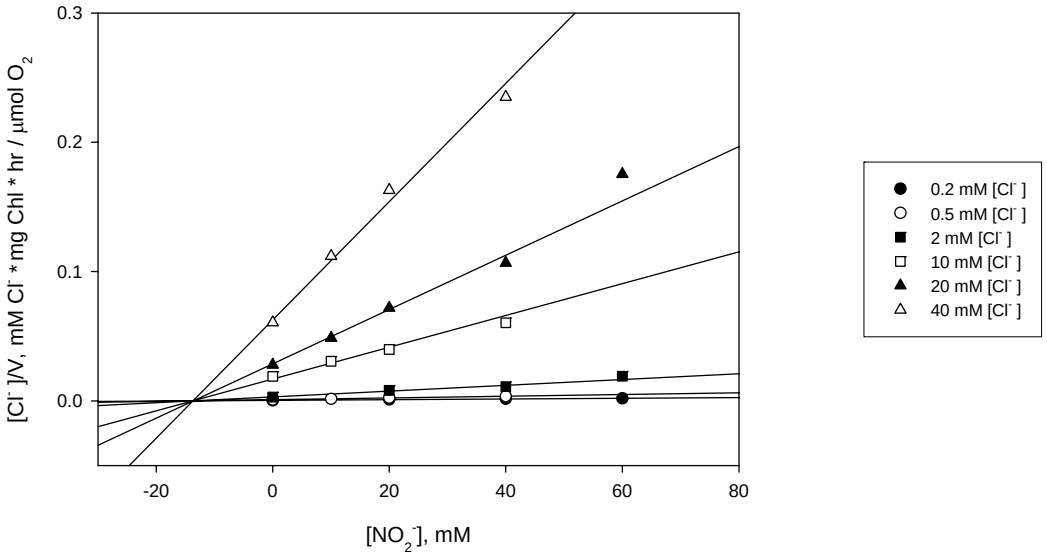

Figure 14 Cornish-Bowden plot for nitrite inhibition of oxygen evolution in intact PSII. The lines represent the fit to the data. The intersection point is (-13.70, 0.000) and K_i' = 14 mM. The data were from M. Kumar.

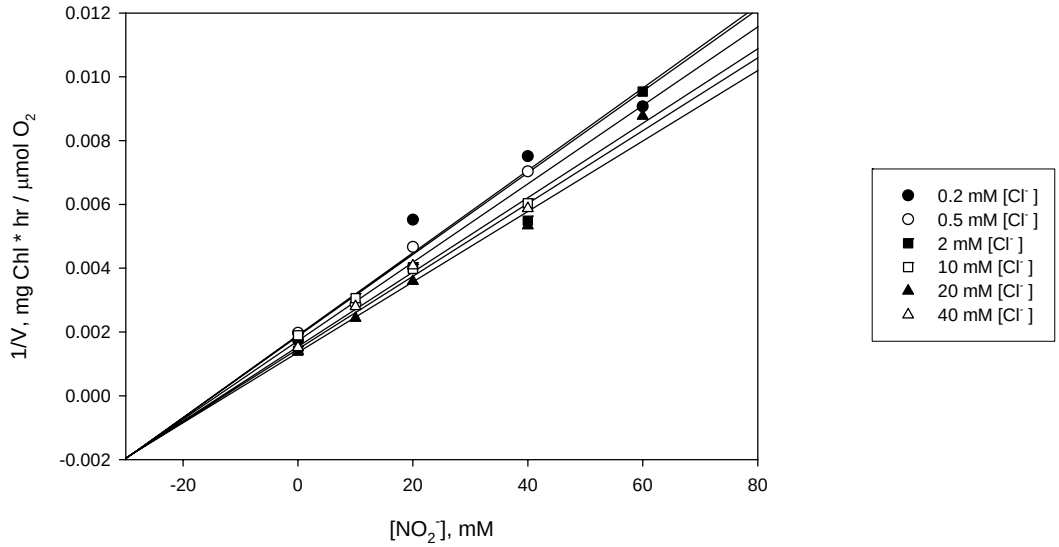

Figure 15 Dixon plot for nitrite inhibition of oxygen evolution in intact PSII. The lines represent the fit to the data. The intersection point is (-28.76, -0.001761) and K_i = 29 mM. The data was from M. Kumar.

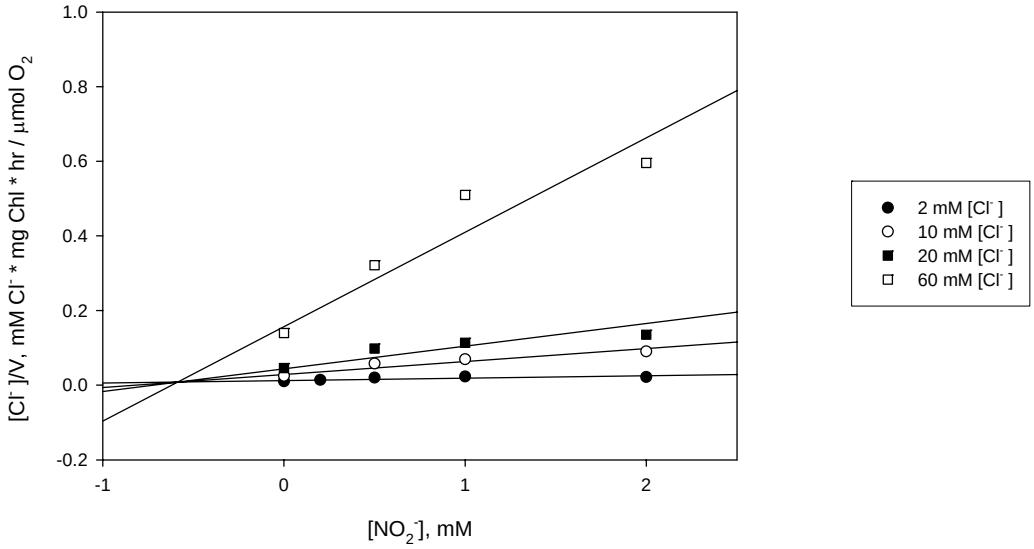

Figure 16 Cornish-Bowden plot for nitrite inhibition of oxygen evolution in NaCl-washed PSII. The lines represent the fit to the data. The intersection point is (-0.5863, 0.008404) and K_i' = 0.6 mM. The data were from M. Kumar.

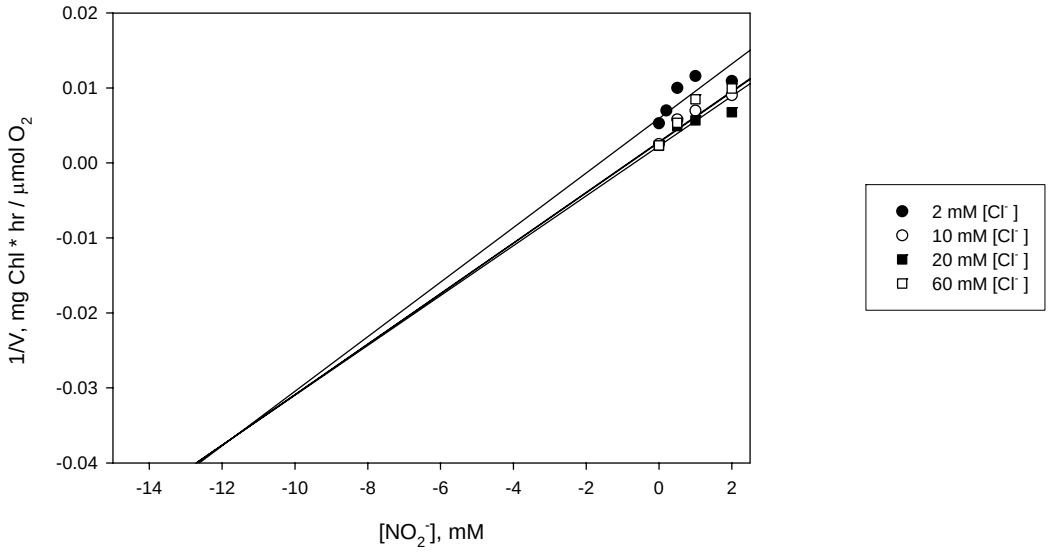

Figure 17 Dixon plot for nitrite inhibition of oxygen evolution in NaCl-washed PSII. The lines represent the fit to the data. The intersection point is (-11.66, -0.03557) and K_i = 12 mM. The data were from M. Kumar.

By comparing the results for intact PSII and NaCl-washed PSII, we observe that K_i' decreased after the loss of the subunits, which means that removal of the 17 and 23 kDa subunits affects the constant. This observation suggests that the uncompetitive site in PSII is revealed more by the removal of the subunits and therefore must be located near the oxygen-evolving complex.

The interesting thing revealed in Figures 16 and 17 is the non-linearity of the data for NaCl-washed PSII at higher NO_2^- concentrations. It is noteworthy that, on the plots of the figures, the data points increase and then slip down with increasing concentration of NO_2^-, which might indicate that NO_2^- is both an inhibitor and an activator depending on the concentration of NO_2^-. If this is true, the kinetic model for NO_2^- is one for inhibition and activation by the same ion, which is similar to the effect of I^-. In fact, a previous study by Wincencjuz et al. suggested that both nitrite and iodide activate oxygen evolution activity.[47] Another research study on I^- effects on O_2 evolution was carried out by Bryson et al. and indicated that I^- had both inhibition and activation effects on intact PSII.[4] The Cornish-Bowden plot from that study revealed that the data points for I^- curved upward instead of downward, as for NaCl-washed PSII for NO_2^- shown in Figures 16 and 17. It has been known that I^- is an

activator when its concentration is lower and an inhibitor when its concentration is higher in intact PSII. NO_2^- may be comparable to I^- with NO_2^- acting as an inhibitor at its lower concentration and an activator at its higher concentration in NaCl-washed PSII. We concluded that more studies were needed on the NO_2^- dependence mode of oxygen evolution due to the non-linearity of the inhibition data.

NO_2^- Dependence of O_2 Evolution in PSII

We carried out an investigation of the NO_2^- activation of oxygen evolution in the absence of added Cl^- for both NaCl-washed PSII and intact Cl^- depleted PSII, from 0 mM through 50 mM nitrite. The results are presented in Figures 18 and 19, which show that NO_2^- has both activation and inhibition effects for each type of PSII. The plots for O_2 evolution rate vs. NO_2^- concentration have a similar appearance to that of I^-,[4] except with a lower level of activation.

Figure 18 represents NO_2^- dependence of oxygen evolution in NaCl-washed PSII. The oxygen evolution rate starts from 20.5 µmol O_2 /mg Chl/hr at 0 mM NO_2^- and increases to about 35.7 µmol O_2/mg Chl/hr at 2 mM NO_2^-, and then it decreases to 23.6 µmol O_2/mg Chl/hr at 50 mM NO_2^-. The activity reaches its peak value between 1 and 5 mM (around 2 mM). This indicates that NO_2^- activates O_2 evolution when its concentration is less than about 2 mM and inhibits the

process when its concentration is greater than about 2 mM. Figure 19 shows NO_2^- dependence of oxygen evolution in intact Cl^- depleted PSII. Because of the high residual Cl^- and/or Br^- that is apparently bound to PSII, the rate begins from about 330 µmol O_2/mg Chl/hr at 0 mM NO_2^- and reaches the peak value of 355 µmol O_2/mg Chl/hr between 0.4 and 1.0 mM NO_2^- (around 0.7 mM), and thereafter, reduces to 88 µmol O_2/mg Chl/hr at 50 mM NO_2^-. It has a similar response mode as in the case of NaCl-washed PSII, but the activation reaches the peak at a lower concentration of nitrite than for NaCl-washed PSII.

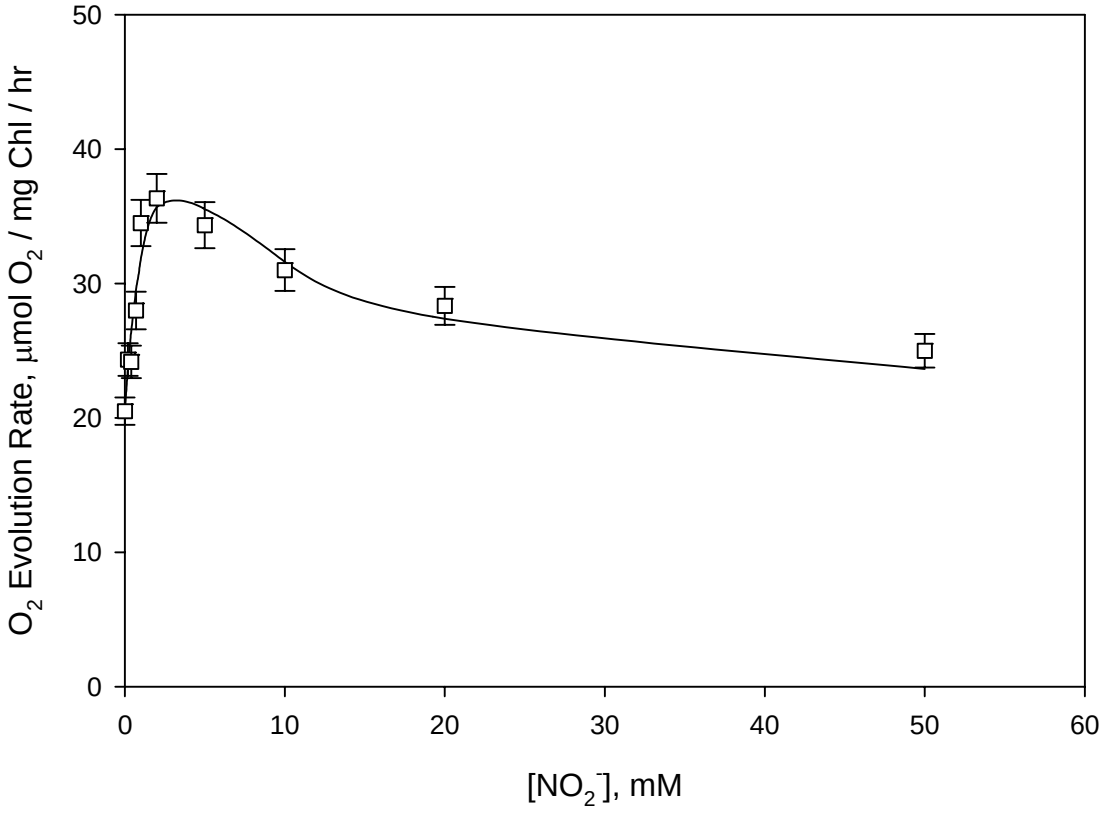

Figure 18 NO_2^- dependence of O_2 evolution rate in NaCl-washed PSII

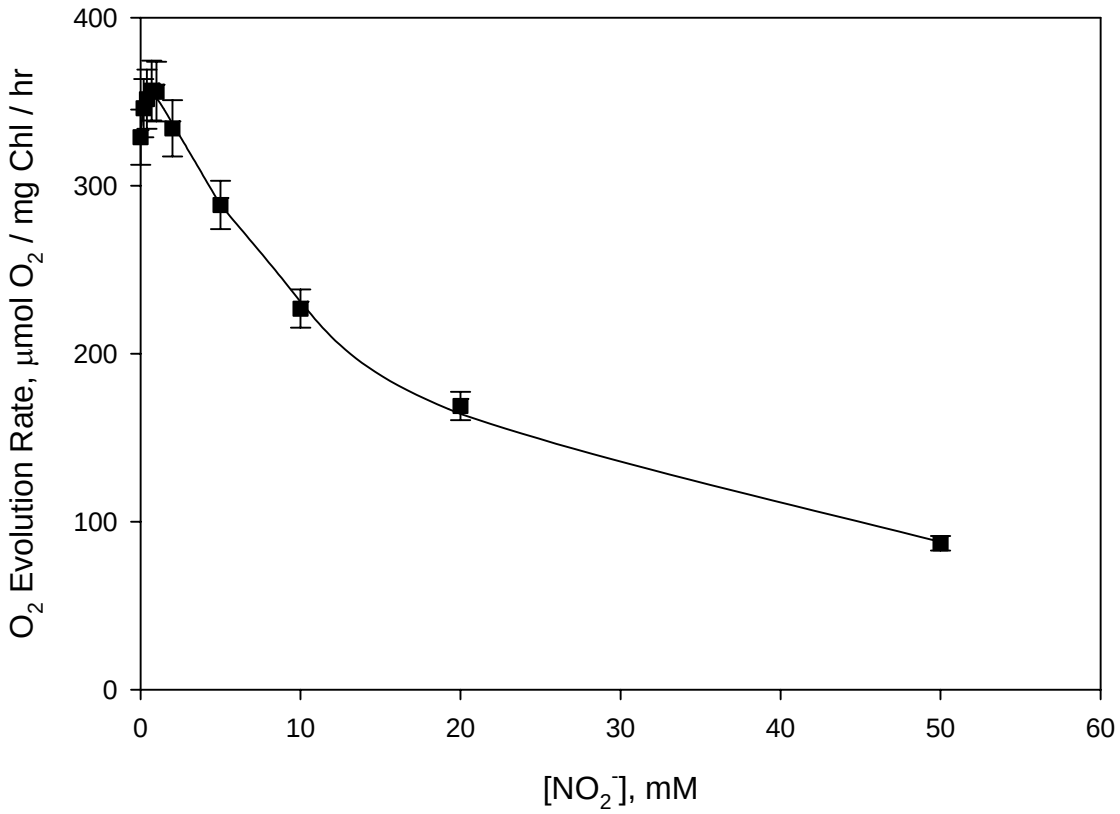

Figure 19 NO_2^- dependence of O_2 evolution rate in intact Cl^- depleted PSII

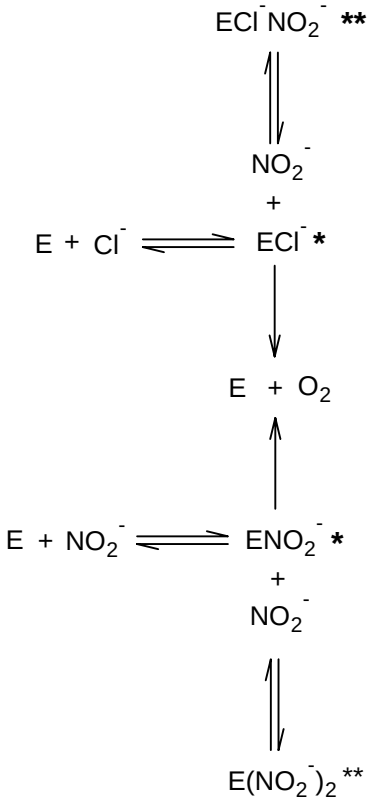

* Activated forms

** Inhibited forms

Reaction 11

NO_2^- acts in PSII by substrate inhibition (activation, and then inhibition), which explains both figures. The reaction scheme for substrate inhibition is shown as in Reaction 11. There are two possible activators (Cl^- and NO_2^-) and one inhibitor (NO_2^-). In the presence of Cl^-, activation by NO_2^- is not likely to be observed. For simplicity, the binding of the true substrate, H_2O, is not shown in the scheme. In the oxygen evolution process, water is present at extremely high concentrations in the medium of PSII (56 M), so is not

limited in availability; Cl^- and NO_2^- bind to the oxygen-evolving reaction sites, resulting in increased activities. As activators, these two anions can be treated as substrates, and consequently, the activation and inhibition kinetics can be treated using the substrate activation and inhibition model with the first substrate (Cl^- or NO_2^-) activating and the second substrate (NO_2^-) inhibiting.[48, 49] The model explains the activation data from this section without Cl^- and the inhibition data from the last section. From this point of view and the equilibria in Reaction 11, the kinetic equations were derived (see Appendix B). The equations refer to the bottom half of the reaction scheme in the absence of Cl^-.

The mathematical expression for the kinetic model of O_2 evolution rate with NO_2^- inhibition in NaCl-washed PSII should be composed of two terms, based on Equation 15:

$$v = \frac{V_{\max}[s]}{K_m + [s] + \frac{[NO_2^-]^2}{K_i}} + V_0 \qquad \textbf{Equation 18}$$

where $[NO_2^-]$ is the concentration of NO_2^-, V_{max} is the maximum evolving velocity promoted by NO_2^-, K_m is the Michaelis constant for activation, and K_i is the dissociation constant for inhibition, and s can be either Cl^- (if it exists) or NO_2^-. The first term represents NO_2^- activation and

inhibition (substrate inhibition). V_0 represents a constant background rate that probably results from residual bound Cl^-. For analysis, V_0 was set to the rate measured at $[NO_2^-]$ = 0 mM. The values found for V_{max}, K_m and K_i are shown in Table 6. The optimal match was reached at R^2 = 0.9204 for the curve fitting.

For intact Cl^- depleted PSII (pretreated with Br^-), because of the high residual O_2 evolving activity from bound Cl^- and/or Br^-, the kinetic model must be treated differently. The high Cl^- and/or Br^- residual activity is inhibited by NO_2^- progressively, so an inhibition term needs to be included in the second term to fully consider the fact. This change matches the data points in Figure 19 where the rate at high $[NO_2^-]$ is much lower than V_0. The complete model gives the equation

$$v = \frac{V_{\max}[s]}{K_m + [s] + \frac{[NO_2^-]^2}{K_i}} + \frac{V_0}{1 + \frac{[NO_2^-]}{K_i}} \qquad \textbf{Equation 19}$$

Again, s can be Cl^- or NO_2^- here. The results of the data analysis are also shown in Table 6. The results showed lower standard errors than those obtained from the analysis for NaCl-washed PSII. R^2 for the curve fitting for intact Cl^- depleted PSII was 0.9991.

Table 6 Comparison of V_{max}, K_m and K_i values for different PSII preparations under NO_2^- inhibition (refer to Figures 18 and 19)

Constant	Intact Cl^- Depleted PSII	NaCl-washed PSII
V_{max} (µmol O_2/mg Chl/hr)	62 ± 6	38 ± 17
K_m (mM)	0.33 ± 0.09	2.1 ± 1.4
K_i (mM)	14.5 ± 0.6	4.5 ± 3.1

From the comparison of NO_2^- dependence of O_2 evolving activity between intact Cl^- depleted and NaCl-washed PSII (Figure 20 and Table 6), we know that the oxygen evolution activity in intact Cl^- depleted PSII is much higher than the activity in NaCl-washed PSII and the inhibition in NaCl-washed PSII is much more evident. The maximum activity for intact Cl^- depleted PSII was about 355 µmol O_2/mg Chl/hr at 0.7 mM NO_2^- while that for NaCl-washed PSII was only 35.7 µmol O_2/mg Chl/hr at 0.7 mM NO_2^-. The former is about 10 times as high as the latter. V_{max} for intact Cl^- depleted PSII is about 1.65 fold as much as that for NaCl-washed PSII. The Michaelis constant for activation (K_m) of NaCl-washed PSII is 6.4 fold as high as that for intact Cl^- depleted PSII. These indicate that the NO_2^- dependent

oxygen evolution activity in intact Cl^- depleted PSII is much higher than that in NaCl-washed PSII. The K_i value for NaCl-washed PSII is much lower than that for intact Cl^- depleted PSII, which means that NO_2^- inhibition is much more significant in NaCl-washed PSII than in intact Cl^- depleted PSII.

Although about 6.5 mM of Ca^{2+} was present during the assays, the O_2 evolution activity of NO_2^- in NaCl-washed PSII was still very low, indicating that the addition of Ca^{2+} did not enhance the activity much. However, under the same conditions, the activity in NaCl-washed PSII can be increased to about 400 µmol O_2/mg Chl/hr by the addition of Cl^-. This can be verified from Figure 21.

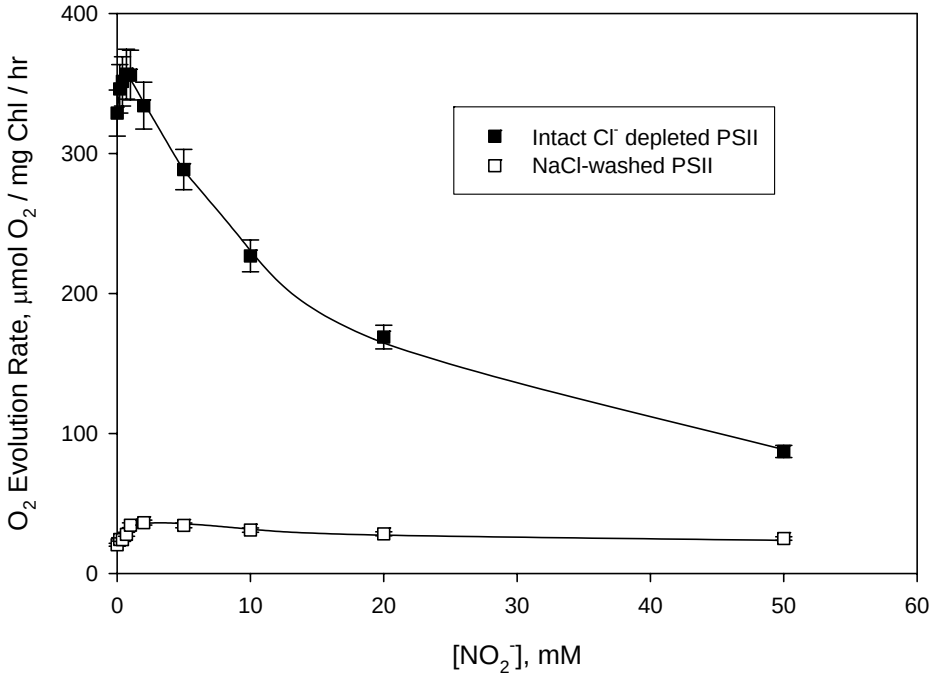

Figure 20 Comparison of NO_2^- dependence of O_2 evolution rate in intact Cl^- depleted PSII vs. in NaCl-washed PSII

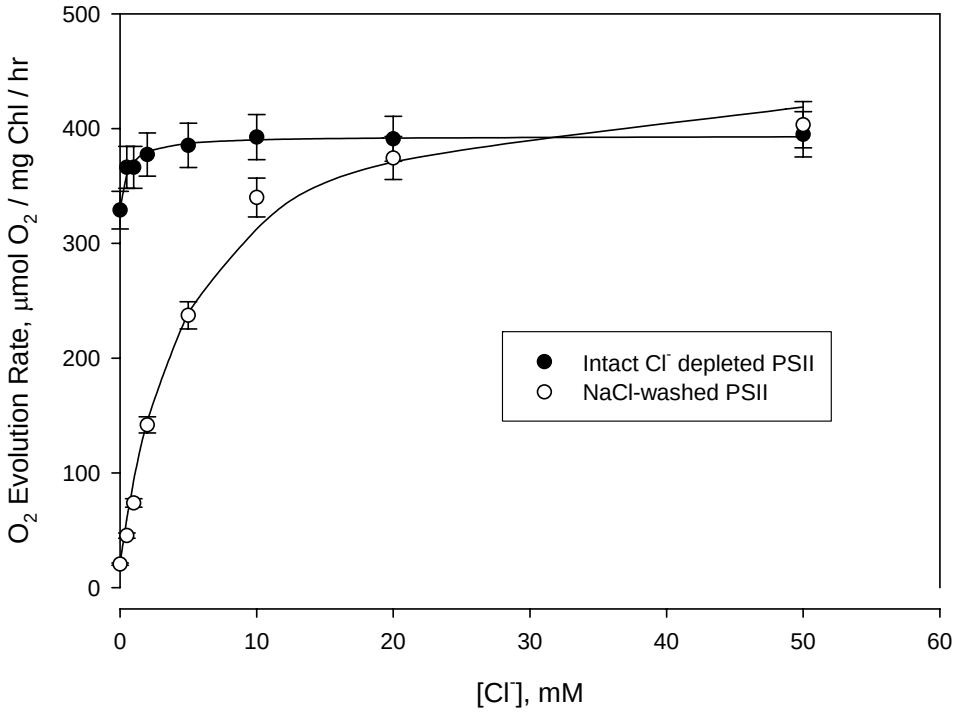

Figure 21 Comparison of Cl^- dependence of O_2 evolution rate in intact Cl^- depleted PSII vs. in NaCl-washed PSII

NO_3^- and Cl^- Dependence of O_2 Evolution in the PSII for the Study

Since Cl^- activation of O_2 evolution has been well studied and reported in many publications before, the comparison of Cl^- activation in PSII used in this research is helpful in understanding the differences between intact Cl^- depleted PSII (pretreated with Br^-) and NaCl-washed PSII. The Cl^- activation kinetic model for both NaCl-washed PSII and intact Cl^- depleted PSII can be written as

$$v = V_0 + \frac{V_{\max}[Cl^-]}{K_m + [Cl^-]} \qquad \text{Equation 20}$$

in which V_0 is the O_2 evolution activity in the absence of added Cl^-. Figure 21 shows the plots for the two types of PSII for Equation 20. The V_{max} and K_m values for Cl^- dependence of O_2 evolution in intact Cl^- depleted and NaCl-washed PSII are shown in Table 7. As for the NO_2^- activation experiments, the initial activity V_0 in intact Cl^- depleted PSII was about 330 μmol O_2/mg Chl/hr, which is very high, and the initial activity V_0 in NaCl-washed PSII was 20.5 μmol O_2/mg Chl/hr, which is quite low. For the Cl^- activation of O_2 evolution in PSII, V_{max} for NaCl-washed PSII was about 6.8 fold of that for intact Cl^- depleted PSII while K_m for NaCl-washed PSII was about 9.3 fold of that for intact Cl^- depleted PSII. At high concentrations of

chloride, the activities for both types of PSII reached around 400 μmol O_2/mg Chl/hr. This indicates that the removal of PsbP and PsbQ from intact PSII did not have a significant effect on the level of full activity.

Table 7 V_{max} and K_m values of NO_3^- and Cl^- Dependence of O_2 Evolution in the PSII

Preparation	Cl^-		NO_3^-		
	V_{max} (μmol O_2/mg Chl/hr)	K_m (mM)	V_{max} (μmol O_2/mg Chl/hr)	K_m (mM)	K_i (mM)
NaCl-washed PSII (With substrate inhibition)	438 ± 19	5.0 ± 0.7	639 ± 216	32.3 ± 13.7	20.6 ± 9.5
NaCl-washed PSII (No substrate inhibition)	438 ± 19	5.0 ± 0.7	183 ± 16	5.5 ± 1.6	N/A
Intact Cl^- depleted PSII	64.6 ± 2.2	0.54 ± 0.10	72.8 ± 9.8	0.16 ± 0.09	97.8 ± 13.4

Due to the similarity of NO_3^- and NO_2^-, the effect of NO_3^- on these two types of PSII was also investigated to facilitate the comparison between these two anions. The same kinetic models for the NO_2^- dependence (Equations 18 and 19) were applied to describe NO_3^- dependence with

substrate inhibition in NaCl-washed PSII and intact Cl^- depleted PSII, respectively. The NO_3^- dependence plots with substrate inhibition are given in Figure 22. The data for NO_3^- dependence were normalized to the data for Cl^- dependence (used as the control data) so that they have the same initial rate with 0 mM of added anions in each type of PSII. The V_{max} and K_m values for NO_3^- dependence of O_2 evolution in intact Cl^- depleted and NaCl-washed PSII with substrate inhibition are shown in Table 7.

However, the data for NaCl-washed PSII showed little substrate inhibition. The curve fitting using Equation 18 resulted in very high V_{max} and K_m values, and the V_{max} value was even higher than that of Cl^-, which was unreasonable. This may result from the lack of data for substrate inhibition, which takes place at high NO_3^- concentrations. Based on this observation, the curve fitting on NO_3^- dependence in NaCl-washed PSII without substrate inhibition was carried out. This fit only involved the activation part of NO_3^- dependence. Using the equation for Cl^- activation (Equation 20), the equation for NO_3^- dependence of O_2 evolution in NaCl-washed PSII without consideration of substrate inhibition became

$$v = V_0 + \frac{V_{\max}[NO_3^-]}{K_m + [NO_3^-]} \qquad \textbf{Equation 21}$$

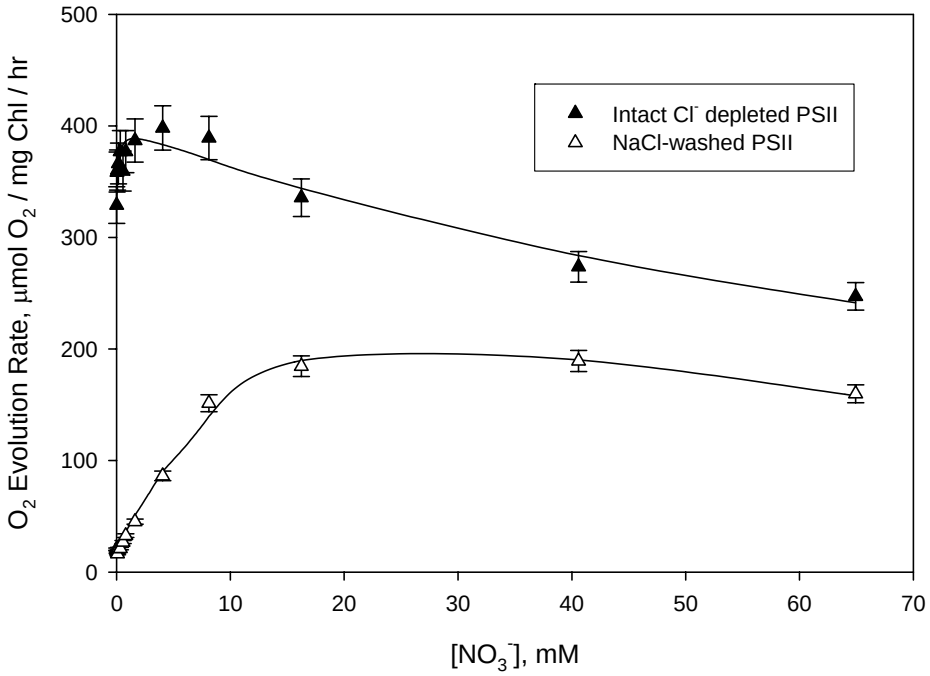

Figure 22 Comparison of NO_3^- dependence of O_2 evolution rate in intact Cl^- depleted PSII vs. in NaCl-washed PSII with substrate inhibition

Its constant values can be found in Table 7 and the plot is shown in Figure 23.

The V_{max} values were 639 and 72.8 μmol O_2/mg Chl/hr for NaCl-washed PSII with substrate inhibition and intact Cl^- depleted PSII, respectively; the former is about 8.8 times as much as the latter. The K_m value for NaCl-washed PSII with substrate inhibition was 196 fold of that for intact Cl^- depleted PSII. The V_{max} and K_m values for NaCl-washed PSII without substrate inhibition were 183 μmol O_2/mg Chl/hr and 5.5 mM, which is about 2.5 and 33 times as high as those of intact Cl^- depleted PSII, respectively. Based on the R^2 values obtained from curve fitting (Table 8), the kinetic expression for NaCl-washed PSII with substrate inhibition (Equation 18) fits the NO_3^- dependence data better than the NO_2^- dependence data, but the expression for intact Cl^- depleted PSII (Equation 19) fits the NO_2^- dependence data better. However, these differences could be due to random errors in the data.

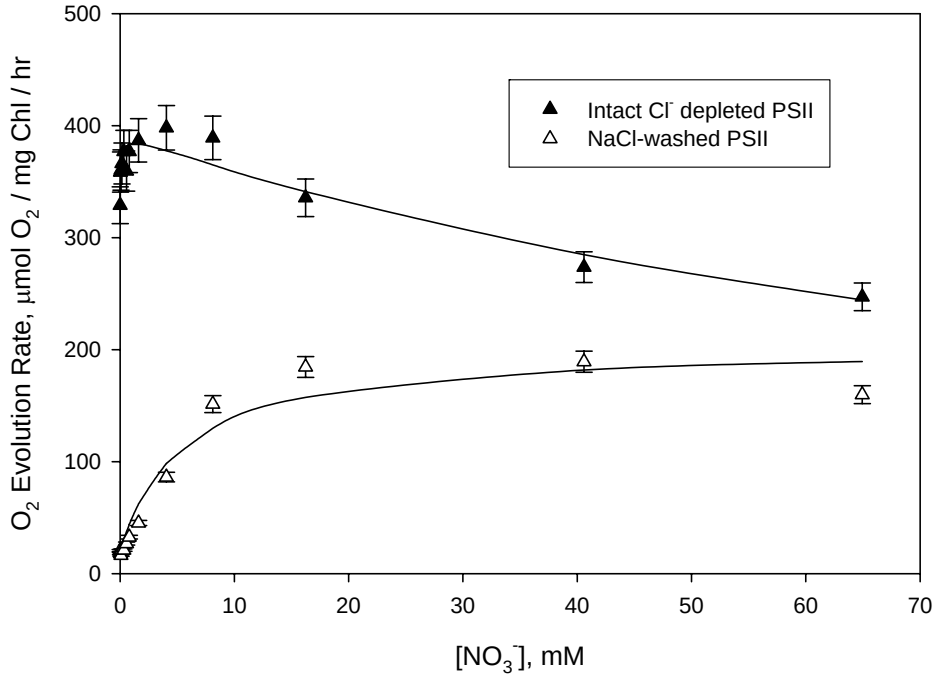

Figure 23 Comparison of NO_3^- dependence of O_2 evolution rate in intact Cl^- depleted PSII vs. in NaCl-washed PSII without substrate inhibition

Table 8 R^2 from regression in fitting the data for NO_2^- and NO_3^- dependence of O_2 evolution rates

Anion	NaCl-washed PSII	Intact Cl^- Depleted PSII
NO_2^-	0.9204	0.9991
NO_3^- (Substrate inhibition)	0.9941	0.9273
NO_3^- (No substrate inhibition)	0.9488	N/A

Comparison of NO_2^-, Cl^- and NO_3^- for Dependence of O_2 Evolution

It is interesting to compare the effect of NO_2^- on the O_2 evolution rate with the effects of Cl^- and NO_3^-. Cl^- is well known as the natural activating anion in the process of oxygen evolution while NO_3^- is an anion close to NO_2^- in chemical characteristics.

In NaCl-washed PSII, the apparent maximum O_2 evolution rates due to NO_2^-, Cl^- and NO_3^- (with substrate inhibition) were 36, 419 and 190 μmol O_2/mg Chl/hr (Figure 24). The highest activity in the presence of NO_2^- was only 8.6% of that due to Cl^- and about 19% of that due to NO_3^-. Chloride activated the oxygen evolution process at all

concentrations tested. When we only consider NO_3^- dependence without substrate inhibition, the mode is similar to that of chloride. The apparent maximum O_2 evolution rate due to NO_3^- was about 190 µmol O_2/mg Chl/hr. As in intact Cl^- depleted PSII, NO_2^- also activated the oxygen evolution process at low concentrations and inhibited at high concentrations in NaCl-washed PSII. However, the activating ability of NO_2^- was much lower than that of NO_3^- and its inhibiting effect was stronger than that of NO_3^-. This can be seen from comparison of the V_{max}, K_m and K_i values in Table 9.

For oxygen evolution in intact Cl^- depleted PSII (see Figure 25), the maximum rates that were reached in the presence of NO_2^-, Cl^- and NO_3^- were 355, 393 and 384 µmol O_2 /mg Chl /hr, respectively. The apparent maximum activity due to Cl^- was higher than that due to NO_3^-; by comparison, the apparent maximum activity of NO_2^- was equal to about 90.3% and 92.4% of those for Cl^- and NO_3^-. Unlike Cl^- which only activated the oxygen evolution process, NO_2^- activated at low concentrations and inhibited at high concentrations. This effect was similar to that of NO_3^-, but its activating ability was a little weaker than NO_3^- while its inhibition effect was much stronger.

All relevant constants are summarized in Table 9. For K_m values, the order from low to high in terms of anions is

NO_3^- < NO_2^- < Cl^- in intact Cl^- Depleted PSII while that in NaCl-washed PSII is NO_2^- < Cl^- < NO_3^- (without substrate inhibition) < NO_3^- (with substrate inhibition). However, the K_m values probably are within error of each other. The V_{max} values for Cl^-, NO_2^- and NO_3^- in NaCl-washed PSII are in the order of NO_3^- (with substrate inhibition) > Cl^- > NO_3^- (without substrate inhibition) > NO_2^-. Those in intact Cl^- Depleted PSII are NO_3^- > Cl^- > NO_2^-, but the differences are small.

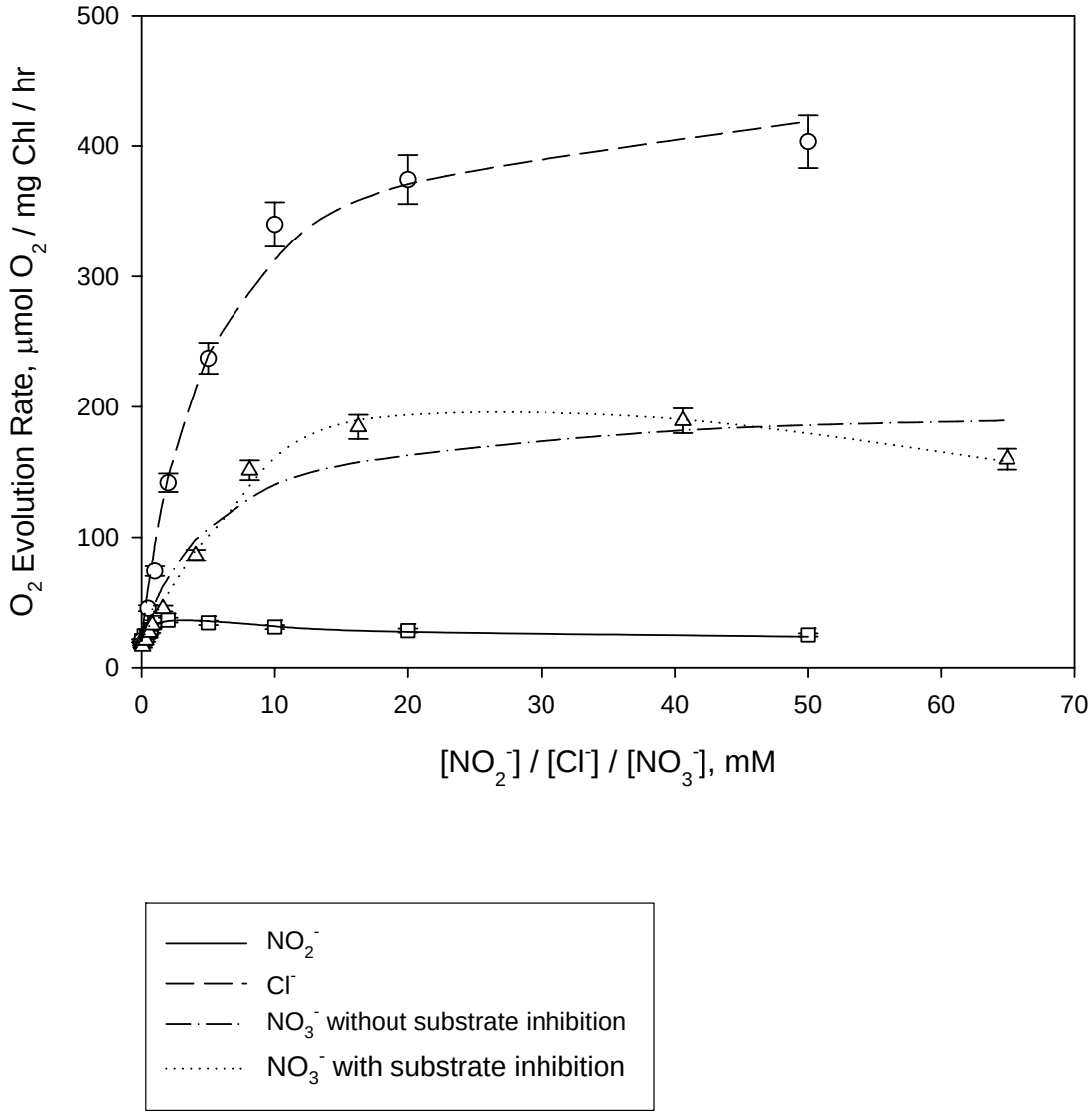

Figure 24 Comparison of anion dependence of O_2 evolution in NaCl-washed PSII

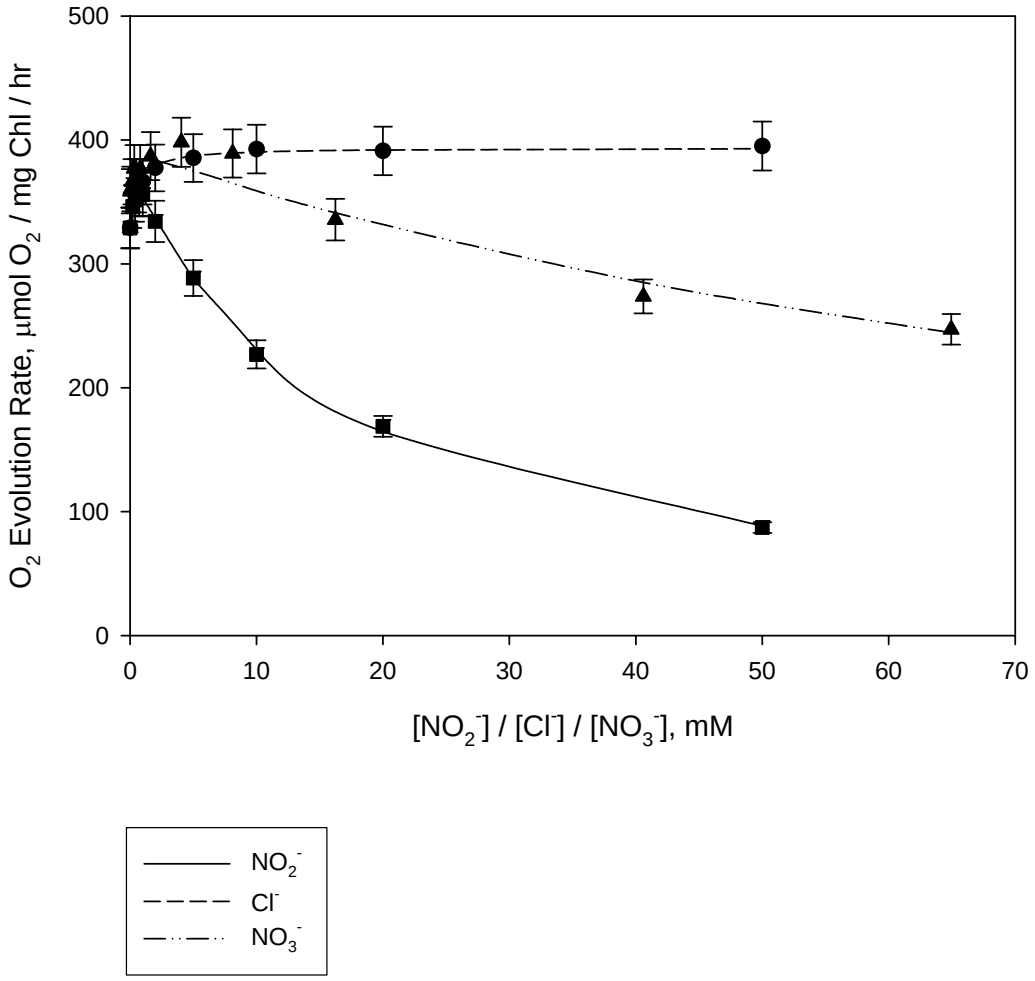

Figure 25 Comparison of anion dependence of O_2 evolution in intact Cl^- depleted PSII

Table 9 Comparison of NO_2^- with NO_3^- and Cl^- for activation and inhibition characteristics

Type of PSII	Constant	Anion Type		
		NO_2^-	NO_3^-	Cl^-
Intact Cl^- Depleted PSII (Prepared by Dialysis with Br^- Pretreatment)	V_{max} (µmol O_2/mg Chl/hr)	62.2	72.8	64.6
	V_0 (µmol O_2/mg Chl/hr)	329	329	329
	K_m (mM)	0.33	0.16	0.54
	K_i (mM)	14.5	97.8	N/A
	$V_{max}+V_0$ (µmol O_2/mg Chl/hr)	391.2	401.8	393.6
	$V_0/(V_{max}+V_0)$	0.841	0.819	0.836
NaCl-washed PSII (With substrate inhibition)	V_{max} (µmol O_2/mg Chl/hr)	38.0	639	438
	V_0 (µmol O_2/mg Chl/hr)	20.5	20.5	20.5
	K_m (mM)	2.1	32.3	5.0
	K_i (mM)	4.5	20.6	N/A
	$V_{max}+V_0$ (µmol O_2/mg Chl/hr)	58.5	659.5	458.5
	$V_0/(V_{max}+V_0)$	0.350	0.031	0.045
NaCl-washed PSII (No substrate inhibition)	V_{max} (µmol O_2/mg Chl/hr)	N/A	183	438
	V_0 (µmol O_2/mg Chl/hr)	20.5	20.5	20.5
	K_m (mM)	N/A	5.5	5.0
	K_i (mM)	N/A	N/A	N/A
	$V_{max}+V_0$ (µmol O_2/mg Chl/hr)	N/A	203.5	458.5
	$V_0/(V_{max}+V_0)$	N/A	0.101	0.045

CHAPTER V

DISCUSSION

Kinetic Models for pH Dependence of O_2 Evolution under F^- Inhibition in Intact PSII

Two mathematical models were established for the pH dependence of the O_2 evolution rate under F^- inhibition in intact PSII. The simplified model is actually a preliminary model for the comprehensive one. Because a number of constants needed to be determined for different fluoride concentrations by nonlinear regression, some problems were encountered in curve fitting due to high interdependence of the parameters and other reasons such as the selection of initial guesses for parameters. The two-step modeling method was designed to reduce the number of parameters and thereby turn a more difficult task into an easier one.

The comprehensive model, as it is named, covers all necessary factors and the essential equilibria between protonation and deprotonation as well as fluoride binding to E, EH, and EH_2. As we have explained, the OEC (E), protons, fluoride and their complexes are involved in equilibria with EH^+ being the active complex for oxygen evolution. In addition to the equilibria for protonation and inhibition as of Reaction 9, we must also consider the reaction scheme from substrate (H_2O) to product (O_2):[50]

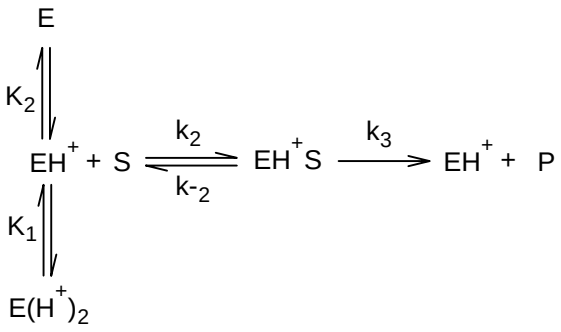

Reaction 12

where P is O_2 and EH^+S is the complex of the active center and the substrate. From these two reaction schemes, the mathematical expression for the comprehensive model can be derived (refer to Appendix A), which is Equation14.

From Figures 12 and 13, we know that the peak of O_2 evolution activity changes with F^- concentration. The peak or the optimal pH shifts to higher pH side when F^- concentration increases. This can be explained by the equilibrium shifting in the scheme of Reactions 8 and 9. In the comprehensive model, K_{i1} has the highest value (380 mM), compared to K_{i0} (16 mM) and K_{i2} (2.0 mM). The dominant species is determined by the concentrations of H^+ and F^- in addition to K_is. K_{i2} is the most important inhibition constant for both the simplified and comprehensive models, because its value is the lowest among those K_is for both cases and it is therefore most sensitive to $[F^-]$ and pH changes. There is no equilibrium for the binding of F^- to E considered in the simplified model, and K_{i1} is the least important in the comprehensive model since it has the

highest value and is least sensitive to the [F^-] and pH changes. K_{i2} represents the low pH side on the plots, and therefore, this part of curve is affected most when F^- concentration increases. Meanwhile, K_{i0} is also significant and represents the high pH side on the plots. The high pH side is also affected some as the concentration of F^- increases. On the other hand, the equilibrium for K_{i2} favors $E(H^+)_2F^-$ formation, causing the equilibrium for K_1 to shift to $E(H^+)_2$ and decreasing the concentration of active EH^+ as the F^- concentration increases. This results in the fluoride inhibition.

A higher concentration of F^- results in increased formation of HF. HF is a weak acid and HCl is a strong acid, and therefore, F^- does not function properly in the H-bonding network if F^- takes the place of Cl^-. As we know, for HF, $K_a = 7.2\times10^{-4}$ or $pK_a = 3.14$. Therefore, the concentrations of F^- in the medium of PSII for various additions of F^- can be easily calculated for different pH values. The following table shows the results for pH 5 and 7.

Table 10 The real concentrations of F^- in PSII solutions after the addition of F^-

Added F^- (mM)	pH = 5	pH = 7
5	4.9 mM	5.0 mM
10	9.9 mM	10.0 mM
15	14.8 mM	15.0 mM
20	19.7 mM	20.0 mM

From the table, we find that the actual concentrations of F^- in PSII are very close to the added concentrations, and fluoride still keeps in the form of F^- ions. At pH 5, the concentrations of F^- are a little lower than the concentrations of added F^- concentrations. At pH 7, the concentrations of F^- have almost no changes from the concentrations of added F^-. This may be related to the observation that F^- inhibition is greater at the lower pH side than at the higher pH side.

Chloride is thought to be a part of hydrogen bond network in PSII, and may participate in protonation stabilizing events through a hydrogen-bonding network during catalysis. The exact binding mode of chloride in PSII is still unclear. However, the OEC functions in a manner similar to other Cl^- activated enzymes. The studies on Cl^- binding to

enzymes may be helpful for us to study Cl^- binding to PSII. For example, Cl^- binding to α-amylase was investigated by Qian et al. using crystallography.[51] The coordination number was found to be 6 for the binding of Cl^-, which changed H-bonding network and caused activation of the enzyme. The pH dependence of α-amylase was also investigated by Numao and coworkers.[52] They found that the pH dependence of α-amylase showed a changing pattern with Cl^- addition similar to the mode for the pH dependence of O_2 evolution under F^- inhibition. Recently, other anion substitutions for Cl^- were also studied on human pancreatic α-amylase.[53] The study showed that many anions, such as Br^-, I^-, NO_2^-, NO_3^-, N_3^- etc., have an activating effect on α-amylase. In PSII, fluoride displaces Cl^- in PSII. Also, F^- can form strong hydrogen bonds that may affect pK_1 or the acidic pK_a value. These factors cause a shift in the optimal pH when the concentration of F^- increases.

In Sandusky's study, the inhibition constants for F^-, K_i and K_i', were about 4 mM and 60-70 mM at pH 7.5;[38] while in Thomas Kuntzleman's research, they were 1.8 mM and 78.7 mM at pH 6.3.[44] In both of the studies, K_i and K_i' were found using Dixon plot and Cornish-Bowden plot, respectively. These K_i values compare well with the K_{i2} value of 2.0 mM F^- found in this study using the comprehensive model. Therefore, we can conclude that K_{i2} is a competitive

inhibition constant. K_{i0} and K_{i1} may be weaker competitive inhibition constants.

The comprehensive model matches the experimental data fairly well, but does not quite encompass the points at high pH accurately. However, the situation was greatly improved compared to the simplified model. Several other more advanced models had been tried to resolve the problem, but all of them required the introduction of more equilibria for E and its complexes with H^+ and F^-, resulting in the use of more parameters. This, in turn, made the modeling more complicated and less likely to fit the data unambiguously. Some of the advanced models can predict the data for higher pH range quite well, but these models were rather difficult to apply using Sigma Plot because too many parameters were introduced. The more complex models may be fitted by holding some parameters constant to test them, but this will need a further study.

Nitrite Inhibition and Activation of O_2 Evolution in PSII

One of the subjects that had been studied was the inhibition mode of nitrite in intact and NaCl-washed PSII. From Figures 14 and 15 which represent intact PSII, it has been noticed that the values of the competitive inhibition constant K_i and the uncompetitive inhibition constant K_i' are fairly closed (29 mM and 14 mM respectively) except

that the error of K_i was very high (243 mM). This means that the inhibition may be actually in the uncompetitive mode because of the large error of K_i. In the case of NaCl-washed PSII as shown in Figures 16 and 17, where K_i = 12 mM (with very high error) and K_i'= 0.6 mM, the inhibition is primarily uncompetitive since K_i is over 10 folds greater than K_i'. That is to say, NO_2^- may function as an uncompetitive inhibitor with respect to chloride activation in both intact and NaCl-washed PSII. It indicates that NO_2^- mainly binds at an uncompetitive site in PSII after Cl^- has bound to PSII. The reason for the high errors of K_i obtained by Kumar is probably that the data don't really show Cl^- activation. The lines for the Dixon plots should be separated better and they would be if the measurements for various Cl^- concentrations at 0 mM of NO_2^- had showed variation in activity.

If we compare the results for intact PSII and NaCl-washed PSII in the study of NO_2^- inhibition modes (Table 5), it can be seen that K_i and K_i' decrease after the loss of 17 and 23 kDa polypeptides. This indicates that removal of the extrinsic subunits affects both constants, but it affects the constant K_i' much more. From this observation, we can conclude that the uncompetitive site in PSII must be revealed more by the removal of the subunits. It also

implies that the site is near the OEC rather than at some other location of PSII.

Because NO_2^- inhibition is uncompetitive in NaCl-washed PSII with activation by Cl^-, the binding of inhibitory NO_2^- will occur after the binding of an activator such as Cl^- or NO_2^-. This implies that NO_2^- inhibition is substrate inhibition in NaCl-washed PSII since uncompetitive inhibition correlates well with substrate inhibition. In the oxygen evolution process, the binding of Cl^- takes place during the S_2 state or an earlier state.[25] So we can conclude that the binding of NO_2^- as an inhibitor should occur after the S_2 state in PsbQ and PsbP depleted PSII membrane with chloride bound. The exact mechanism of this effect needs other detection tools, such as EPR spectroscopy, to be revealed.

Another subject under investigation was the nitrite dependence of the oxygen evolution rate in NaCl-washed PSII and intact Cl^- depleted PSII. NO_2^- was known to both activate and inhibit oxygen evolution process in these two types of PSII membranes. It activates the evolution process at low concentrations and inhibits the process at higher concentrations, similar to some other monovalent anions such as I^- and NO_3^-.[3, 4] Like I^- and NO_3^-, NO_2^- activates oxygen evolution in both intact Cl^- depleted PSII and NaCl-wash PSII, which indicates that the 17 and 23 kDa extrinsic

subunits (or PsbQ and PsbP) do not prevent NO_2^- access to the activating site on PSII membrane. [54, 55] Its inhibitory effect on O_2 evolution is also much larger than I^- and NO_3^-.

The reaction scheme of the kinetic models for both types of PSII was determined to be like that in Reaction 11. Since NO_2^- activates (at low concentrations) and inhibits (at higher concentrations) O_2 evolving activity, either NO_2^- or Cl^- bind to the activating site of OEC as a first step, then NO_2^- binds to the enzyme complex at the inhibiting site. There is a K_m for activation promoted by each anion, NO_2^- or Cl^-. For both NaCl-washed PSII and intact Cl^- depleted PSII, NO_2^- acts as an activator binding on E at first and then as an inhibitor by binding on ENO_2^-. The derivation of the mathematical expressions is presented in Appendix B.

Equations 18 and 19 are the mathematical models describing NO_2^- activation and inhibition in the PSII. The results show that these models predict the experimental data quite well except the fit for NO_3^- in NaCl-washed PSII with substrate inhibition that has an unreasonably high V_{max} value (Table 9). All PSII membranes used in the studies were Cl^- deficient because they were either Cl^- depleted and/or were washed with chloride-free buffer.

Thus, a conclusion can be made that, in the absence of chloride, the dependence of O_2 evolution on NO_2^- is

activation followed by inhibition in both types of PSII and that there are two activators (Cl^- and NO_2^-) and one inhibitor (NO_2^-). The NO_2^- inhibition mode is uncompetitive in NaCl-washed PSII, and is probably uncompetitive in intact PSII also, given the high error of the data. It would be very helpful to fully understand the inhibition mode of NO_2^- in intact Cl^- depleted PSII if a study of the topic is performed.

A lower K_m (0.33 mM) for NO_2^- activation in intact PSII, compared to a higher K_m (2.1 mM) for NO_2^- activation in NaCl-washed PSII, indicates that the extrinsic subunits (PsbP and PsbQ) have the function of holding NO_2^- that activates the oxygen evolution process. In addition, K_i for intact Cl^- depleted PSII (14.5 mM) is over 3 times higher than K_i for NaCl-washed PSII (4.5 mM). This indicates that the removal of PsbP and PsbQ polypeptides results in a stronger inhibiting effect, which implies that the inhibition site is closer to the OEC and the OEC was protected from NO_2^- inhibition by these two extrinsic subunits.[4]

The R^2 for oxygen evolution dependence on NO_2^- in intact Cl^- depleted PSII and NO_3^- in NaCl-washed PSII with substrate inhibition are 0.9991 and 0.9941, respectively. They are close to one, which indicates that the equation for substrate inhibition in NaCl-washed PSII (Equation 18)

predicts the experimental data for NO_3^- dependence accurately; also, the equation for substrate inhibition in intact Cl^- depleted PSII (Equation 19) fits the related data on NO_2^- dependence excellently. However, since the fit for NO_3^- in NaCl-washed PSII with substrate inhibition resulted in an unreasonably high V_{max} value, the model without substrate inhibition was used. The R^2 is 0.9488, which is not very high, but it was reasonable given the problem with the fit including substrate inhibition. R^2 for the dependence on NO_2^- in NaCl-washed PSII was only 0.9204. This fit was probably subject to systematic errors in the measuring process because of the extremely low activity of NO_2^- in NaCl-washed PSII, even though the PSII was incubated and kept in chloride-free buffer containing about 6.5 mM of Ca^{2+}. At such low activities, O_2 evolution rates were very difficult to be determined accurately. An interesting observation is that Equation 19 also did not predict the data for the dependence on NO_3^- in intact Cl^- depleted PSII accurately, as we noted that R^2 was only 0.9273 for the regression. This observation can be easily seen from Figure 22, where the peak area is not well modeled. The meaning of this is probably that NO_3^- and NO_2^- may have different modes or mechanisms of activation and inhibition in intact Cl^- depleted PSII (prepared by dialysis with pretreatment of Br^-). Such observation was also found in other studies.[5] One

possible reason for the lower R^2 of some fits may be that a portion of the V_0 activity is not able to be inhibited, moving the effective baseline up from zero.

So far, we have seen that NaCl-washed PSII has much lower O_2 evolution activity than intact PSII, and that NaCl-washed PSII needs Ca^{2+} to work properly. The reason that we use NaCl-washed PSII so often is that the studies on NaCl-washed PSII are more informative than intact PSII because of much less interference from residual Cl^-. Also, Cl^- is easier to remove from NaCl-washed PSII than from intact PSII.

NO_2^- versus NO_3^- and Cl^- on Activation and/or Inhibition

V_{max}, K_m and K_i data for each anion are summarized in Table 9.

1. In intact Cl^- depleted PSII.

As we note the maximal activities V_{max} of all three anions are 64.6, 62.2 and 72.8 μmol O_2/mg Chl/hr for Cl^-, NO_2^- and NO_3^- in intact Cl^- depleted PSII, respectively. The values are closer to each other if the errors are considered. K_m values for them are fairly close because they are all within the error range. Therefore, it is difficult to compare the activating effects of these anions from the data. This may be because V_0 is so high, resulting in higher errors in the activation portions. The K_i value of

NO_2^- is much lower than that of NO_3^- with substrate inhibition, indicating that NO_2^- has much stronger inhibiting effect on O_2 evolution.

2. In NaCl-washed PSII.

The V_{max} of NO_2^-, Cl^-, NO_3 with substrate inhibition and NO_3 without substrate inhibition for NaCl-washed PSII are 38.0, 438, 639 and 183 μmol O_2/mg Chl/hr, respectively. The order of V_{max} from high to low is: NO_3^- with substrate inhibition > Cl^- > NO_3^- without substrate inhibition > NO_2^-, which means that NO_2^- has a very weak activating effect in NaCl-washed PSII. The pure activating effect of Cl^- is higher than that of NO_3^- without substrate inhibition. The V_{max} for NO_3^- with substrate inhibition was found when there were not enough data at higher concentrations obtained in the study, so the value cannot be count for the comparison. Meanwhile, NO_3^- has some inhibiting effect and this may be the part of the reason why the apparent maximum activity is lower than that of Cl^-.

On the other hand, K_m values of NO_2^-, Cl^-, NO_3^- with substrate inhibition and NO_3^- without substrate inhibition for NaCl-washed PSII are 2.1, 5.0, 32.3 and 5.5 mM. The values for NO_2^-, Cl^-, and NO_3^- without substrate inhibition are fairly close and all are within the error range except for that of NO_3^- with substrate inhibition. The V_{max} value of Cl^- is higher than that of NO_3^- without substrate inhibition

and the K_m value is lower than that of NO_3^- without substrate inhibition, which indicates that Cl^- has the highest activating effect among the anions. This also means that NO_3^- promotes oxygen evolution activity at a higher concentration than Cl^- does in NaCl-washed PSII.

3. Inhibition effects.

The lower K_i values of NO_2^- represent that it is a very strong inhibitor as compared to NO_3^-. The reason may be that NO_2^- has strong ligand field strength while the strength for NO_3^- is weak, and therefore, the NO_2^- binding at the inhibiting sites is stronger than that of NO_3^-. Also, it may be related to the fact that HNO_2 is a weak acid while HNO_3 is a very strong acid. The K_a of HNO_2 is 4.5×10^{-4}. NO_2^- is likely to affect H-bonding more than NO_3^-.

The K_i value for intact Cl^- depleted PSII in the study of nitrite dependence was 14.5 mM which is very close to the K_i' value for intact PSII in the study of nitrite inhibition (14.0 mM). The result implies that substrate inhibition and uncompetitive inhibition are well correlated in intact PSII. In Stemler's study on bicarbonate-reversible and irreversible inhibition of photosystem II by NO_2^- using a thylakoid preparation, the K_d (K_i) values were found to be 0.264 mM and 0.481 mM, respectively, when the concentration of NO_2^- was 5 and 10 mM.[40] The large differences of the K_i values are because the PSII used in this research was from

spinach thylakoids and the one in Stemler's study was from maize thylakoids. The most important factor was that Stemler's study consisted of two inhibitors, nitrite and bicarbonate at pH 7.6, and therefore, showed much lower inhibition constants. Since substrate inhibition correlates well with uncompetitive inhibition, it implies that nitrite is an uncompetitive inhibitor and binds at a site other than the active site in intact PSII. Moreover, Cl^- depletion has no significant effect on the nitrite inhibition mode in intact PSII.

Activators or inhibitors of oxygen evolution bind at different sites, including active, competitive inhibition and uncompetitive inhibition sites of Cl^-. Figure 26 represents a schematic diagram of the binding sites of Cl^- and other anions competing with Cl^- discussed in this research. In the figure, the active (or competitive inhibition) site is depicted to be close to the Mn_4-Ca cluster. It can be bound by activators such as Cl^-, NO_3^-, NO_2^- and I^-, and by competitive inhibitors like F^-. The uncompetitive inhibition site is depicted to be close to the extrinsic subunits, and can be bound by the uncompetitive inhibitors such as NO_3^-, NO_2^-, I^-, etc. The uncompetitive site might be able to bind Cl- in a nonfunctional way.

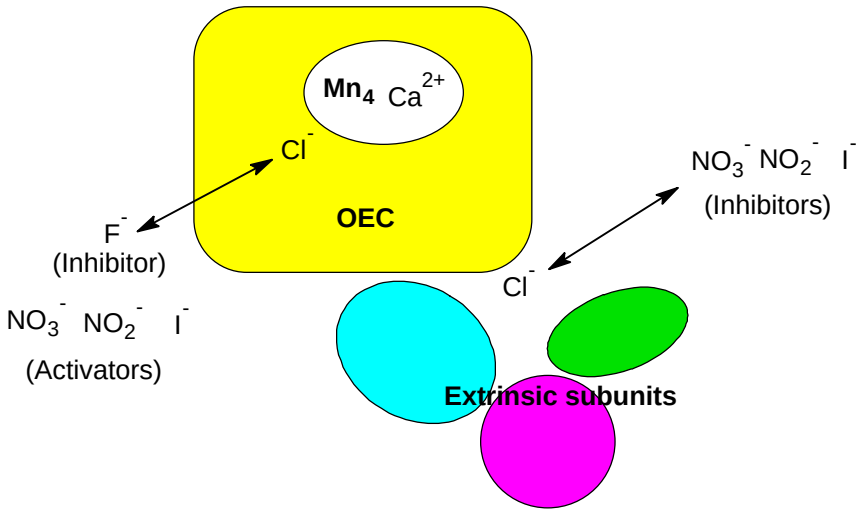

Figure 26 Schematic diagram of the possible binding sites of activators and inhibitors

CHAPTER VI

CONCLUSION

In the first part of the studies, a comprehensive kinetic model for the pH dependence of oxygen evolution rate with fluoride inhibition in intact PSII was established, and in general, the kinetic constants determined for the mathematical expression can predict the experimental data quite well. There is no research on such models that has been published before. However, although fairly good, the model did not predict the oxygen evolution rates at higher pH very accurately; for instance, the plots for pH >7.5 do not represent the experimental data well. This is probably due to some reason(s) that has not been discovered or the model itself may need to be improved further. Additional efforts had been focused on solving this problem, but all efforts required models with more parameters, which introduced problems in finding unique solutions. Further studies should be carried out to address this topic by performing more experiments.

Nitrite activation and inhibition effects on oxygen evolution were also investigated in the research. Based on the data obtained by Kumar et al, the NO_2^- inhibition modes in intact PSII and NaCl-washed PSII were found, which is that NO_2^- may be an uncompetitive inhibitor for both types

of PSII. However, this conclusion is made based on the large error of the competitive inhibition constant in intact PSII. The reason for the large errors is probably that the data obtained by Kumar did not really show Cl^- activation. This should be studied in the future.

The research on NO_2^- dependence of oxygen evolution revealed that NO_2^- activated the oxygen evolution process at lower concentrations but inhibited the process at high concentrations in intact Cl^- depleted PSII and NaCl-washed PSII. In the experiments for both types of PSII, the kinetic models are similar to those for iodide.[4]

REFERENCES

1. William J. Coleman. "Chloride binding proteins: mechanistic implications for the oxygen-evolving complex of photosystem II". *Photosynthesis Research*, 1990, 23, 1-27.

2. Kenneth Olesen and Lars-Erik Andréasson. "The function of the chloride ion in photosynthetic oxygen evolution". *Biochemistry*, 2003, 42, 2025-2035.

3. Peter H. Homann. "Chloride and calcium in photosystem II: from effects to enigma". *Photosynthesis research*, 2002, 73, 169-175.

4. David I. Bryson, Ninad Doctor, Rachelle Johnson, Sergei Baranov, and Alice Haddy. "Characteristics of iodide activation and inhibition of oxygen evolution by photosystem II". *Biochemistry*, 2005, 44, 7354-7360.

5. Xiaoming Li. "Investigation of dialysis methods for the complete removal of Cl^- from photosystem II". *Thesis for the Degree of Master of Science*, The University of North Carolina at Greensboro, 2006, 24-25.

6. Peter H. Homann. "The chloride and calcium requirement of photosynthetic water oxidation: effects of pH". *Biochimica et Biophysica Acta*, 1988, 934, 1-13.

7. Christopher K. Mathews and K. E. van Holde. "Chapter 19, Photosynthesis". *Biochemistry*, 1990, The Benjamin/Cummings Publishing.

8. Veronika A. Szalai and Gary W. Brudvig. "How plants produce dioxygen". *American Scientist*, 1998, 86, 542-551.

9. Cecie Starr and Ralph Taggart. *Biology, The Unity and Diversity of Life,* 4^{th} edition, 1987, Wadsworth Publishing Company.

10. Warwick Hillier and Gerald T. Babcock. "Photosynthetic reaction centers". *Plant Physiology*, 2001, 125, 33-37.

11. Athina Zouni, Horst-Tobias Witt, Jan Kern, Petra Fromme, Norbert Krauβ, Wolfram Saenger, and Peter Orth. “Crystal structure of photosystem II from *Synechococcus elongates* at 3.8 Å resolution”. *Nature*, 2001, 409, 739-743.

12. Nobuo Kamiya and Jian-Ren Shen. “Crystal structure of oxygen-evolving photosystem II from Thermosynechococcus vulcanus at 3.7 Å resolution”. *PNAS*, 2003, 100, 98-103.

13. Bernhard Loll, Jan Kern, Wolffram Saenger, Athina Zouni, and Jacek Biesiadka. “Towards complete cofactor arrangement in the 3.0 Å resolution structure of photosystem II”. *Nature*, 2005, 438, 1040-1044.

14. Terry M. Bricker and Demetrios F. Ghanotakis. “Chapter 8, Introduction to oxygen evolution and the oxygen-evolving complex”. *Oxygenic Photosynthesis: The Light Reaction by Donald R. Ort and Charles F. Yocum*, 1996, Kluwer Academic Publishers, Netherlands, 113-136.

15. Christa Critchley. “The role of chloride in photosystem II”. *Biochimica et Biophysica Acta*, 1985, 811, 33-46.

16. Lars-Gunnar Franzén, Örjan Hansson, and Lars-Erik Andréasson. “The rolesof the extrinsic subunits in photosystem II as revealed by EPR”. *Biochimica et Biophysica Acta*, 1985, 808, 171-179.

17. Kristina N. Ferreira, Tina M. Iverson, Karim Maghlaoui, James Barber, and So Iwata. “Architecture of the photosynthetic oxygen-evolving center”. *Science*, 2004, 303, 1831-1838.

18. R. David Britt. “Chapter 9, Oxygen evolution”. *Oxygenic Photosynthesis: The Light Reactions by Donald R. Ort; Charles F. Yocum*, 1996, Kluwer Academic Publishers, Netherlands, 137-164.

19. Archna Sahay, Anjana Jajoo, and Sudhakar Bharti. “A thermoluminescence study of the effects of nitrite on photosystem II in spinach thylakiods”. *Luminescence*, 2006, 21, 143-147.

20. A. W. Rutherford and A. Boussac. “Water photolysis in biology”. *Science*, 2004, 303, 1782-1784.

21. Curtis W. Hoganson and Gerald T. Babcock. "A metalloradical mechanism for the generation of oxygen from water in photosynthesis". *Science*, **1997**, 277, 1953-1956.

22. Hans J. van Gorkom and Charles F. Yocum. "Chapter 13, The calcium and chloride cofactors". *Photosystem II: The Light-Driven Water: Plastoquinone Oxidoreductase by T. Wydrzynski and K. Satoh*, **2005**, Springer, Netherlands, 307-327.

23. Jan Kern, Jacek Biesiadka, Bernhard Loll, Wolfram Saenger, and Athina Zouni. "Structure of the Mn_4-Ca cluster as derived from X-ray diffraction". *Photosynthesis Research*, **2007**, 92, 389-405.

24. M. Miqyass, H. J. van Gorkom, and C. F. Yocum. "The PSII Calcium site revisited". *Photosynthesis Research*, **2007**, 92, 275-287.

25. Vittal K. Yachandra, R.D. Guiles, Kenneth Sauer, and Melvin P. Klein. "The state of manganese in the photosynthetic apparatus. 5. The chloride effects in photosynthetic oxygen evolution. Is halide coordinated to the EPR-active manganese in the O_2-evolving complex? Studies of the substructure of the low-temperature multilane EPR signal". *Biochimica et Biophysica Acta*, **1986**, 850, 333-342.

26. M. Baumgarten, J. S. Philo, and G. C. Dismukes. "Mechanism of photoinhibition of photosynthetic water oxidation by Cl^- depletion and F^- substitution: oxidation of a protein residue". *Biochemistry*, **1990**, 29, 10814-10822

27. Katrin Lindberg and Lars-Erik Andreasson. "A one-site, two-state model for the binding of anions in photosystem II". *Biochemistry*, **1996**, 35, 14259-14267.

28. Katrin Lindberg, Tore Vanngard, and Lars-Erik Andreasson. "Studies of the slowly exchanging chloride in photosystem II of higher plants". *Photosynthesis Research*, **1993**, 38, 401-408.

29. Victoria J. DeRose, Matthew J. Latimer, Jean-Luc Zimmermann, Ishita Mukerji, Vittal K. Yachandra, Kenneth Sauer, and Melvin P. Klein. "Fluoride substitution in the Mn cluster from photosystem II: EPR and X-ray absorption spectroscopy studies". *Chemical Physics*, **1995**, 194, 443-459.

30. Alice Haddy, J. Andrew Hatchell, R. Allen Kimel, and Rebecca Thomas. "Azide as a competitor of chloride in oxygen evolution by photosystem II". *Biochemistry*, **1999**, 38, 6104-6110.

31. Alice Haddy, R. Allen Kimel, and Rebecca Thomas. "Effects of azide on the S_2 state EPR signals from photosystem II". *Photosynthesis Research*, **2000**, 63, 35-45.

32. Taka-Aki Ono, Haruto Nakayama, Herman gleiter, Yorinao Inoue, and Asako Kawamori. "Modification of the properties of S_2 state in photosynthetic O_2-evolving center by replacement of chloride with other anions". *Archieves of Biochemistry and Biophysics*, **1987**, 256, 618-624.

33. Deborah A. Berthold, Gerald T. Babcock, and Charles F. Yocum. "A highly resoved, oxygen-evolving photosystem II preperation from spinach thylakiod membranes". *FEBS Letters*, **1981**, 134, 231-234.

34. Mitsue Miyao and Norio Murata. "Partial disintegration and reconstitution of the photosynthetic oxygen evolution system". *Biochimica et Biophysica Acta*, **1983**, 725, 87-93.

35. M. Dixon. "The determination of enzyme inhibitor constants". *Biochemical Journal*, **1953**, 55, 170-171.

36. Athel Cornish-Bowden. "A simple graphical method for determining the inhibition constants of mixed, uncompetitive and non-competitive inhibitors". *Biochemical Journal*, **1974**, 137, 143-144.

37. Peter O. Sandusky and Charles F. Yocum. "The chloride requirement for photosynthetic oxygen evolution. Analysis of the effects of chloride and other anions on amine inhibition of the oxygen-evolving complex". *Biochimica et Biophysica Acta*, **1984**, 766, 603-611.

38. P.O. Sandusky and C.F. Yocum. "The chloride requirement for photosynthetic oxygen evolution: factors affecting nucleophilic displacement of chloride from the oxygen-evolving complex". *Biochimica et Biophysica Acta*, **1986**, 849, 85-93.

39. H. Spiller and P. Böger. "Photosynthetic nitrite reduction by dithioerythritol and the effect of nitrite on electron transport in isolated chloroplasts". *Photochemistry and Photobiology*, **1971**, 26, 397-402.

40. A. J. Stemler and J. B. Murphy. "Bicarbonate-reversible and irreversible inhibition of photosystem II by monovalent anions". *Plant Physiology*, **1985**, 77, 974-977.

41. Koji Hasegawa, Yulihiro Kimura, and Taka-aki Ono. "Chloride cofactor in the photosynthetic oxygen-evolving complex studied by Fourier transform infrared spectroscopy". *Biochemistry*, **2002**, 41, 13839-13850.

42. R. C. Ford and M. C. W. Evans. "Isolation of a photosystem 2 preparation from higher plants with highly enriched oxygen evolution activity". *FEBS Letters*, **1983**, 160, 159-164.

43. Daniel I. Arnon. "Copper enzymes in isolated chloroplasts. Polyphenoloxidase in beta vulgaris". *Plant Physiology*, **1949**, 24, 1-15.

44. Thomas S. Kuntzleman. "Fluoride inhibition and the role of the 17 kDa and 23 kDa extrinsic polypeptides in calcium and chloride activation in photosystem II". *Thesis for the Degree of Master of Science*, The University of North Carolina at Greensboro, **2000**, 33-34.

45. *Sigma Plot 2000 User's Guide,* Revised Edition, **2000**.

46. *Sigma Plot 2000 Programming Guide,* Revised Edition, **2000**.

47. Hanna Wincencjusz, Charles F. Yocum, and Hans J. Van Gorkom. "Activating anions that replace Cl^- in the O_2-evolving complex of photosystem II slow the kinetics of the terminal step in water oxidation and destabilize the S_2 and S_3 states". *Biochemistry*, **1999**, 38, 3719-3725.

48. A. R. Schulz. *Enzyme Kinetics: From Diastase to Multienzyme Systems*, **1994**, Cambridge University Press, Cambridge.

49. A. Cornish-Bowden. *Fundamentals of Enzyme Kinetics*, **1995**, Portland Press, London.

50. Athel Cornish-Bowden and Christopher W. Wharton. *Enzyme Kinetics*, 1988, IRL Press Limited, Oxford.

51. Minxie Qian, El Hassan Ajandouz, Françoise Payan, and Virginie Nahoum. "Molecular basis of the effects of chloride ion on the acid-base catalyst in the mechanism of pancreatic α-amylase". *Biochemistry*, 2005, 44, 3194-3201.

52. Shin Numao, Robert maurus, Gary Sidhu, Yili wang, Christopher M. Overall, Gary D. Brayer, and Stephen G. Withers. "Probing the role of the chloride ion in the mechanism of human pancreatic α-amylase". *Biochemistry*, 2002, 41, 215-225.

53. Robert Maurus, Anjuman begum, Leslie K. Williams, Jason R. Fredriksen, Ran Zhang, Stephen G. Withers, and Gary D. Brayer. "Alternative catalytic anions differentially modulate human α-amylase activity and specificity". *Biochemistry*, 2008, 47, 3332-3344.

54. A. Seider. "The extrinsic polypeptides of photosystem II". *Biochimica et Biophysica Acta*, 1996, 1277, 35-60.

55. M. Miyao and N. Murata. "The Cl^- effect on photosynthetic oxygen evolution: interaction of Cl^- with 18-kDa, 24-kDa, and 33-kDa proteins". *FEBS Letter*, 1985, 180, 303-308.

APPENDIX A

DERIVATION OF KINETIC EXPRESSIONS OF pH DEPENDENCE OF OXYGEN EVOLUTION UNDER FLUORIDE INHIBITION IN INTACT PSII

Kinetic Expression for pH Dependence of O_2 Evolution without F^-

The equilibria for the pH dependence of oxygen evolution without inhibition can be expressed as

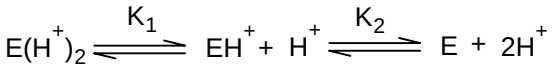

Reaction A1

where E, EH^+ and $E(H^+)_2$ are the oxygen evolving center and its protonated complexes, in which EH^+ is the active center. The reaction to produce O_2 is [45]

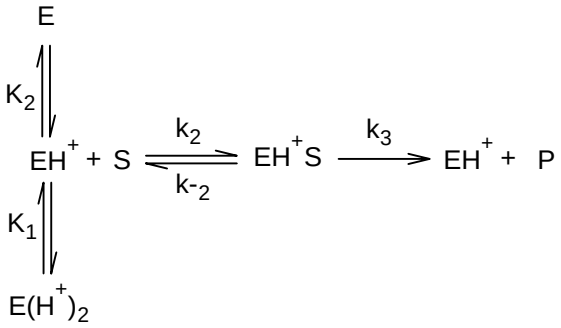

Reaction A2

where P is the product, which is O_2 here. Since the rate-determining step in the above scheme is the one involving k_3 and the substrate S (which is water) is in an extremely excess amount, the reaction velocity can be expressed as

$$v = \frac{d[P]}{dt} = k[EH^+] \qquad \textbf{Equation A1}$$

Here, k is the constant that includes k_2, k_{-2} and k_3. The protonation equilibria are given by

$$K_1 = \frac{[H^+][EH^+]}{[E(H^+)_2]} \qquad \textbf{Equation A2}$$

$$K_2 = \frac{[H^+][E]}{[EH^+]} \qquad \textbf{Equation A3}$$

The total concentration of E and its complexes is

$$E_{total} = [E] + [EH^+] + [E(H^+)_2] \qquad \textbf{Equation A4}$$

By converting Equations A2 and A3 into the expressions for [E] and $[E(H^+)_2]$ in terms of $[EH^+]$, followed by insertion into Equation A4, we have

$$E_{total} = [EH^+]\left[1 + \frac{[H^+]}{K_1} + \frac{K_2}{[H^+]}\right] \qquad \textbf{Equation A5}$$

Observing that

$$\frac{A}{A_{\max}} = \frac{[EH^+]}{E_{total}} \qquad \textbf{Equation A6}$$

the kinetic expression for the model of the pH dependence of oxygen evolution without inhibition in intact PSII can be found to be

$$A = \frac{A_{max}}{1 + \frac{[H^+]}{K_1} + \frac{K_2}{[H^+]}} \qquad \textbf{Equation A7}$$

Kinetic Expression for the Simplified Model of pH Dependence of Oxygen Evolution under F^- Inhibition

Because F^- inhibition equilibria for EH^+ and $E(H^+)_2$ are more significant than that for E, we can establish a simplified model of the pH dependence of oxygen evolution with F^- inhibition in intact PSII. This model has the equilibrium schemes shown as Reactions A2 and A3.

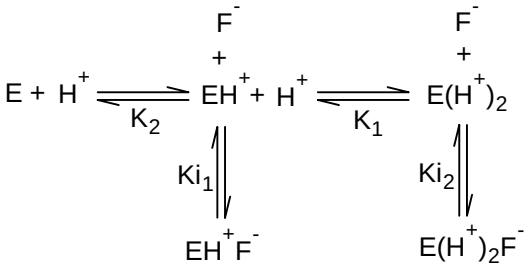

Reaction A3

where EH^+F^- and $E(H^+)_2F^-$ are inhibited complexes. The oxygen evolution activity can still be expressed using Equation A1. Equations A2 and A3 are the expressions for K_1 and K_2. From Reaction A3, we also have

$$K_{i1} = \frac{[F^-][EH^+]}{[EH^+F^-]}$$ **Equation A8**

$$K_{i2} = \frac{[F^-][E(H^+)_2]}{[E(H^+)_2F^-]}$$ **Equation A9**

The total concentration of E and its complexes is

$$E_{total} = [E]+[EH^+]+[E(H^+)_2]+[EH^+F^-]+[E(H^+)_2F^-]$$ **Equation A10**

If we convert Equations A2, A3, A8 and A9 into the expressions for [E], $[E(H^+)_2]$, $[EH^+F]$ and $[E(H^+)_2F]$ in terms of $[EH^+]$, and then insert them into Equation A10, the following equation can be obtained.

$$E_{total} = [EH^+]\left\{1+\frac{[H^+]}{K_1}+\frac{K_2}{[H^+]}+[F^-]\left(\frac{1}{K_{i1}}+\frac{[H^+]}{K_1K_{i2}}\right)\right\}$$ **Equation A11**

Using Equations A6 and A11, we obtain the mathematical expression of the simplified model for the pH dependence of O_2 evolution rate on F^- inhibition in intact PSII, which is

$$A = \frac{A_{\max}}{1+\frac{[H]}{K_1}+\frac{K_2}{[H]}+[F]\left(\frac{1}{K_{i1}}+\frac{[H]}{K_1K_{i2}}\right)}$$ **Equation A12**

Here [F] is the concentration of F^-. K_{i1} and K_{i2} are the dissociation constants of fluoride inhibition for EH^+F^- and $E(H^+)_2F^-$ respectively.

Kinetic Expression for the Comprehensive Model of pH Dependence of Oxygen Evolution under F^- Inhibition

For a comprehensive model, the reaction scheme is

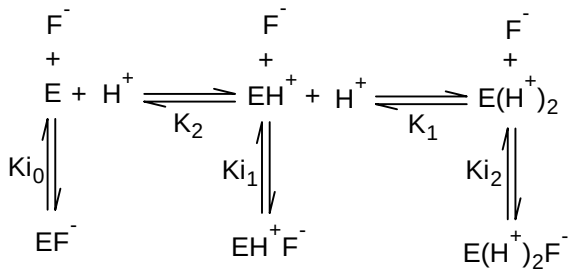

Reaction A4

At the same time, Reaction A2 presents the reaction to produce the final product, P or O_2. Equation A1 can still be applied here, and also, k is the constant that includes k_2, k_{-2}, and k_3. From Reaction A4, we have

$$K_{i0} = \frac{[F^-][E]}{[EF^-]} \qquad \textbf{Equation A13}$$

The total concentration of E and its complexes is

$$E_{total} = [E] + [EH^+] + [E(H^+)_2] + [EF^-] + [EH^+F^-] + [E(H^+)_2F^-] \qquad \textbf{Equation A14}$$

Upon converting Equations A2, A3, A8, A9 and A13 into the expressions for [E], $[E(H^+)_2]$, $[EF^-]$, $[EH^+F]$ and $[E(H^+)_2F]$ in

terms of $[EH^+]$, followed by insertion into Equation A14; we have

$$E_{total} = [EH^+]\left\{1 + \frac{[H^+]}{K_1} + \frac{K_2}{[H^+]} + [F^-]\left(\frac{1}{K_{i1}} + \frac{[H^+]}{K_1 K_{i2}} + \frac{K_2}{K_{i0}[H^+]}\right)\right\} \qquad \textbf{Equation A15}$$

Given Equation A6, the rate becomes

$$A = \frac{A_{\max}}{1 + \frac{[H]}{K_1} + \frac{K_2}{[H]} + [F]\left(\frac{1}{K_{i1}} + \frac{[H]}{K_1 K_{i2}} + \frac{K_2}{K_{i0}[H]}\right)} \qquad \textbf{Equation A16}$$

which is the mathematical expression of the comprehensive model for the pH dependence of O_2 evolution rate on F^- inhibition in intact PSII.

APPENDIX B

DERIVATION OF EXPRESSIONS OF NITRITE AND NITRATE DEPENDENCE OF OXYGEN EVOLUTION IN NaCl-WASHED AND INTACT Cl^- DEPLETED PSII

Both NO_2^- and NO_3^- activate and then inhibit the oxygen evolution, and therefore, the same model can be used for both. Let us use NO_2^- for the derivation. Since Cl^- also activates PSII, there is a K_m for activation promoted by each anion, NO_2^- or Cl^-. In both NaCl-washed PSII and intact Cl^- depleted PSII, NO_2^- acts as an activator binding on E at first and then as an inhibitor by binding on ENO_2^-. The equilibrium scheme is

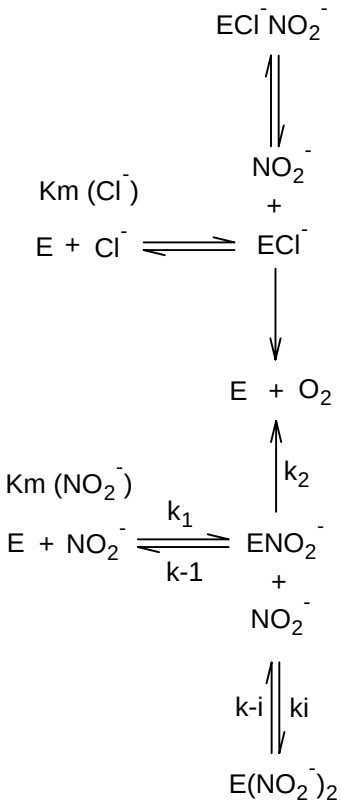

Reaction B1

We assume that the reactions are at the steady state. The kinetic expressions may be derived as follows.[48] From Reaction B1, we have

$$\frac{d[E]}{dt} = -k_1[E][NO_2^-] + (k_{-1} + k_2)[ENO_2^-] = 0 \qquad \textbf{Equation B1}$$

and

$$\frac{d[E(NO_2^-)_2]}{dt} = k_i[ENO_2^-][NO_2^-] - k_{-i}[E(NO_2^-)_2] = 0 \qquad \textbf{Equation B2}$$

Equations B1 and B2 can be rearranged into

$$[E] = \frac{K_m[ENO_2^-]}{[NO_2^-]} \qquad \textbf{Equation B3}$$

$$[E(NO_2^-)_2] = \frac{[ENO_2^-][NO_2^-]}{K_i} \qquad \textbf{Equation B4}$$

in which $K_m = (k_{-1}+k_2)/k_1$, and $K_i = k_{-i} / k_i$. The total concentration of E and E complexes would be

$$E_{total} = [E]+[ENO_2^-]+[E(NO_2^-)_2] = [ENO_2^-](1+\frac{K_m}{[NO_2^-]}+\frac{[NO_2^-]}{K_i})$$

Equation B5

Since $v = k_2[ENO_2^-]$, we have

$$v = \frac{k_2 E_{total}}{1+\frac{K_m}{[NO_2^-]}+\frac{[NO_2^-]}{K_i}} = \frac{V_{\max}[NO_2^-]}{K_m+[NO_2^-]+\frac{[NO_2^-]^2}{K_i}} \qquad \textbf{Equation B6}$$

Where $V_{max} = k_2E_{total}$. For NaCl-washed PSII, the residual activity was very low, so an additional term V_0 was added to the kinetic model to express it and the inhibition effect on V_0 was neglected. Therefore, the kinetic expression is

$$v = \frac{V_{\max}[NO_2^-]}{K_m + [NO_2^-] + \frac{[NO_2^-]^2}{K_i}} + V_0$$ **Equation B7**

In the case of intact Cl^- depleted PSII dialyzed with Br^- pretreatment, the residue activity from Cl^- and/or Br^- was high, and therefore, the inhibition effect on V_0 was included. Then,

$$v = \frac{V_{\max}[NO_2^-]}{K_m + [NO_2^-] + \frac{[NO_2^-]^2}{K_i}} + \frac{V_0}{1 + \frac{[NO_2^-]}{K_i}}$$ **Equation B8**

This is the mathematical equation for the kinetic model of NO_2^- dependence of oxygen evolution in intact Cl^- depleted PSII.[4]

Since NO_3^- has a similar behavior as NO_2^- in oxygen evolution, Equations B7 and B8 can be applied to express the NO_3^- dependence of oxygen evolution in NaCl-washed PSII with substrate inhibition and intact Cl^- depleted PSII, respectively.